Chemical Engineering Journal 547 (2026) 180884

Contents lists available at ScienceDirect

Chemical Engineering Journal

journal homepage: www.elsevier.com/locate/cej

Review

Conductive hydrogels under extreme environments: From material design to application

Yuying Wu [a,*,1], Cifang Jiang [b,1], Gang Zhou [c,*], Xinyuan Zhu [d], Youfu Wang [d,*]

[a] School of Electrical and Energy Engineering, Shanghai DianJi University, Shanghai, 201306, PR China
[b] School of Materials Science and Engineering, Shanghai Dianji University, Shanghai, 201306, PR China
[c] Key Laboratory of Integrated Regulation and Resources Development on Shallow Lakes, Ministry of Education, College of Environment, Hohai University, Nanjing, 210098, PR China
[d] School of Chemistry and Chemical Engineering, Frontiers Science Center for Transformative Molecules, Shanghai Jiao Tong University, Shanghai, 200240, PR China

ARTICLE INFO

Keywords:
Conductive hydrogels
Environmental adaptability
Extreme environments
Flexible sensors

ABSTRACT

Conductive hydrogels combine a hydrated polymer network with tunable mechanical and electrical properties, making them promising soft interfaces for flexible electronics. However, the high water content of hydrogels poses significant challenges under extreme service environments, such as freezing at low temperatures, water loss under arid conditions, excessive swelling in high humidity, chemical corrosion, mechanical degradation under large deformation, and physical damage. All these factors severely limit the performance stability and operational lifetime of hydrogel-based electronic devices. To address these bottlenecks, this review first systematically analyzes the failure mechanisms of conductive hydrogels in five typical extreme environments: low temperature, arid conditions, high humidity, corrosive environments, and large mechanical deformation. Subsequently, from the perspective of materials design, this review categorizes and summarizes recent advances in adaptive protection strategies, including anti-freezing, anti-drying, anti-swelling, anti-corrosion, and stretchability, with a particular focus on enhancement mechanisms such as dynamic bonding and nanocomposite reinforcement. On this basis, focusing on flexible strain, pressure, and temperature sensors, this review discusses the implementation pathways by which the aforementioned strategies ensure signal sensitivity, repeatability, linear response, and long-term operational stability under extreme environments. Finally, this review focuses on conductive hydrogel sensing materials. It addresses the trade-offs and conflicting requirements in their design. Current challenges in this area are summarized. Future directions are also proposed, including tolerance to multiple coupled environments, green manufacturing, and closed-loop life-cycle assessment. The goal is to offer a theoretical and technical foundation for developing high-performance sensors for extreme conditions.

1. Introduction

Rapid advances in artificial intelligence (AI), soft robotics, and human-computer interaction have increased the demand for wearable and flexible electronic devices, placing higher performance requirements on the core flexible conductive materials. Specifically, edge AI applications, precise actuation of soft robots, and unobtrusive human-computer interaction all demand flexible materials that simultaneously exhibit good flexibility, electrical conductivity, and biocompatibility, in order to resolve the mismatch between traditional rigid materials and biological tissues, thereby providing core support for the development of wearable electronic devices. Over the past decade, wearable flexible electronic devices have been widely used in various fields, such as health monitoring [1–3], flexible energy harvesting and storage [4–7], human-machine interfaces [8–11], soft robotics [12,13], precision therapy [14,15], owing to their portability and adaptability to different surfaces. However, traditional flexible materials, such as the natural flexible material cellulose, despite their excellent mechanical properties and tunability, ease of functionalization, and outstanding biocompatibility and biodegradability [16], also exhibit significant drawbacks including high brittleness, poor flexibility and elasticity, and insufficient thermal stability [17], all of which lead to unstable performance of the related products. With the in-depth research and exploration of wearable flexible electronic devices, the high modulus, non-deformability, and

* Corresponding authors.
E-mail addresses: wyy2021h@163.com (Y. Wu), gangzhou@hhu.edu.cn (G. Zhou), wyfown@sjtu.edu.cn (Y. Wang).
[1] These authors contributed equally to this work.

https://doi.org/10.1016/j.cej.2026.180884
Received 15 June 2026; Received in revised form 6 August 2026; Accepted 17 August 2026
Available online 18 August 2026
1385-8947/© 2026 Published by Elsevier B.V.

geometric rigidity of traditional rigid materials constitute a fundamental contradiction against the soft, dynamic, and morphologically irregular characteristics of biological tissues [18]. In contrast, wearable electronic devices based on flexible materials offer significant advantages in terms of flexibility, stretchability, and breathability, enabling biomimetic conformal integration with human tissues and surpassing the limitations of rigid materials [19–21]. This has effectively given rise to emerging fields such as electronic skin and soft robotics, serving as a key driver for the development of human-machine integration and bio-integrated electronics [22].

Hydrogels are promising soft materials because their high hydration and mechanical compliance resemble those of biological tissues. They are characterized by a hydrated three-dimensional (3D) polymer network and tissue-compatible mechanical properties [23–25], which endow them with effective performance at bioelectronic interfaces. Their tissue-compatible composition and compliance make them particularly suitable for skin-conformal adhesion, while their hydrated network imparts high elasticity and toughness. Moreover, the 3D network, which manifests as a porous structure, can be engineered into stimuli-responsive materials for intelligent modulation, offering both good permeability and favorable mass transport [26]. Consequently, hydrogels, as a class of flexible materials, hold broad application prospects in fields such as biomedicine, tissue engineering, drug delivery, and flexible electronics [27–31]. Incorporating mobile ions or electronically conductive components further enables rapid electrical signal transmission while preserving the mechanical compliance of the hydrated network [32–35]. Here, several representative milestones are summarized in Fig. 1 to illustrate the development of conductive-hydrogel sensing. The key events are selected to outline the main trajectory of conductive hydrogel-based sensing applications.

However, despite the considerable attention that the remarkable properties of conductive hydrogels have attracted from researchers, their high water content renders them highly sensitive to environmental fluctuations [36–38], thereby impeding their stability under certain extreme conditions. In this review, extreme environments are defined as environmental conditions under which conductive hydrogels can no longer maintain stable structural integrity, mechanical properties, electrical conductivity, or sensing performance. Based on the dominant failure mechanisms of hydrated polymer networks, five representative categories of extreme environments are considered, such as low

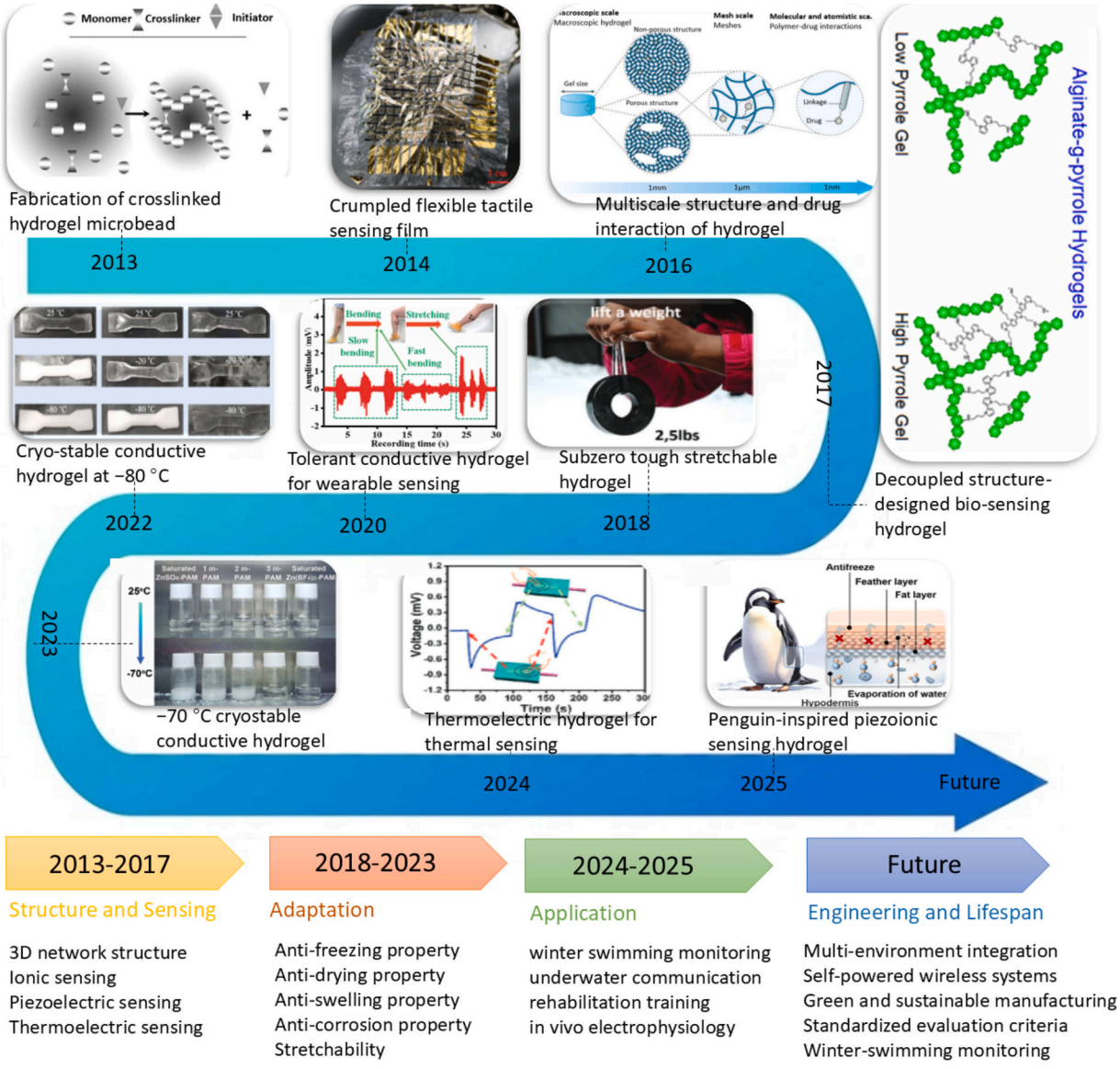


Fig. 1. Evolution of conductive hydrogels from structural design and sensing mechanisms to environmental adaptation, multifunctional applications, and future development.

temperature, arid conditions, high humidity, corrosive environments, and large mechanical deformation. Low-temperature environments generally refer to subzero conditions, typically below 0 °C. Representative studies have investigated temperatures ranging from −20 °C to −80 °C, under which ice formation can severely restrict ion mobility and mechanical flexibility. Arid conditions correspond to low-humidity environments, typically at a relative humidity (RH) below 30%, or continuous dehydration conditions causing water loss and network shrinkage. High-humidity environments generally refer to RH >80%, where excessive moisture absorption induces swelling and dimensional instability. Corrosive environments include acidic solutions (typically pH <5), alkaline solutions (typically pH >9), high ionic-strength solutions with salt concentrations typically exceeding 1 M, and organic solvents that disrupt polymer interactions. Large mechanical deformation generally refers to tensile strains exceeding 100%, where irreversible network damage and sensing degradation may occur. Because the critical exposure duration varies with hydrogel composition and application scenario, long-term exposure means continuous operation or storage under extreme conditions until measurable degradation occurs in mechanical, electrical, or sensing performance. For example, at or below −2 °C, the freezing of free water within the hydrogel leads to a decrease in ion mobility, accompanied by pronounced hardening and embrittlement of the hydrogel material, resulting in loss of flexibility and degradation of electromechanical performance. Meanwhile, the formation of ice crystals also reduces the mobile free medium within the hydrogel, diminishing its permeability and electrical conductivity [39,40]. This implies that ice crystals within the hydrogel severely restrict the application of flexible wearable electronic devices in cold environments [41]. Similarly, under arid conditions or high-temperature environments, rapid water evaporation from hydrogel causes its network structure to shrink and collapse, disrupting its original porous architecture. As a result, the original porous 3D structure is disrupted and difficult to maintain. Moreover, water molecules act like plasticizers within the hydrogel, keeping the polymer chains flexible. Upon water loss, chain segment motion is hindered, and the material becomes stiff and brittle [42,43]. Under high-humidity conditions, hydrogels absorb moisture from the air through their 3D network structure, leading to a significant increase in volume, which may result in decreased dimensional accuracy of devices, reduced sensor sensitivity, and diminished adhesion of the hydrogel [44]. When immersed in corrosive solutions for long-term exposure, hydrogels typically suffer performance failure due to the disruption of their three-dimensional polymer network. In strongly acidic or alkaline solutions, the chemical bonds within the hydrogel may undergo hydrolytic cleavage, leading to dissolution of the hydrogel. Similarly, in high-concentration salt solutions and organic solvents, the interactions between polymer chains in the hydrogel are weakened, ultimately resulting in the destruction of the hydrogel structure, which may lead to partial loss of functionality [45,46]. When a hydrogel undergoes large tensile deformation, its internal polymer network experiences a transition from entropic elasticity-dominated reversible extension to irreversible structural damage. When deformation exceeds the critical strain of the hydrogel, structural damage occurs. This is due to insufficient stretchability. The resulting loss of function puts the wearable device at risk of tearing or mechanical failure [47].

Recent studies have examined hydrogel-based sensing materials from several complementary perspectives. Molecular interactions, network architecture, and structure-property relationships have been summarized to establish the fundamental principles governing hydrogel design and performance regulation [48]. Dynamic crosslinking and self-healing mechanisms have also been reviewed as routes to mechanically adaptive networks capable of stress relaxation and functional recovery [49,50]. Other studies have focused on hydrogels resistant to harsh environments, particularly anti-freezing, anti-drying, and water-management strategies [51,52], whereas hydrogel-based flexible and self-powered sensing platforms have been discussed in the context of wearable electronics and human-machine interfaces [53]. Collectively, these reviews provide an important foundation for the development of functional hydrogels. Nevertheless, the connections among environmentally induced failure, adaptive material design, signal transduction, retention of sensing performance under service conditions, and engineering translation remain fragmented. In particular, a unified framework is still needed to explain how conductive hydrogels fail under specific extreme environments, how structural and compositional regulation suppresses the corresponding failure processes, whether this protection is translated into stable electrical signals and sensing performance, and what barriers prevent laboratory-scale advantages from being transferred to practical devices.

To address this need, this review establishes a continuous framework linking "environmental failure-adaptive design-signal transduction-service performance-engineering translation" (Fig. 2). First, we analyze the dominant failure mechanisms under various extreme conditions, including low temperature, arid environments, aqueous or high-humidity exposure, corrosive media, and large mechanical deformation. Corresponding strategies, namely anti-freezing, anti-drying, anti-swelling, anti-corrosion, and stretchability enhancement are then discussed. Second, resistance-based, piezoionic, thermoresistive, and ionic thermoelectric transduction are distinguished according to their physical origins, stimulus conditions, and electrical outputs. Finally, the barriers to engineering translation, including manufacturing scalability, device reliability, packaging, standardization, and commercialization, are critically discussed. Through these interconnected levels, the review moves beyond a property-by-property summary and provides a service-oriented framework for evaluating conductive hydrogel sensors under extreme environments.

2. Microstructure and transduction mechanisms

Conductive hydrogels combine a hydrated polymer network with ionic, electronic, or hybrid conductive pathways. Their sensing behavior is governed not only by bulk electrical conductivity but also by how external stimuli and service environments regulate network geometry, carrier mobility, water activity, ion distribution, conductive-component contacts, and hydrogel-electrode interfaces. These coupled changes are converted into measurable resistance, current, or voltage signals. Mechanically induced electrical outputs require particular distinction, as exemplified by flexible piezoelectric materials that generate bound polarization charge through strain-induced polarization of a non-centrosymmetric or explicitly piezoelectric phase [54]. Whereas ionically conductive hydrogels can generate piezoionic signals through the redistribution of mobile ions. Accordingly, we first introduce the polymer sources, crosslinking modes, and ionic, electronic, and hybrid conductive components that establish the hydrated network and charge-transport basis. Then, we subsequently discuss transduction under mechanical deformation, temperature variation, humidity/water exposure, and chemical/corrosive media, followed by coupled stimuli and signal interpretation. Within these service-related categories, resistance-based, piezoionic, thermoresistive, and ionic thermoelectric transduction pathways are distinguished according to their physical origins, electrical outputs, and applicable quantitative descriptors.

2.1. Microstructure of conductive hydrogels

Conductive hydrogels are hydrated polymer networks characterized by a 3D structure. Their hydrophilic backbone enables the uptake and retention of substantial water. This network architecture is primarily formed by chemical or physical crosslinking between polymer chains.

2.1.1. Polymer sources of conductive hydrogels

Conductive hydrogels can be constructed from natural polymer sources, synthetic sources, or a combination of both, and their electrical conductivity is imparted by introducing conductive components.

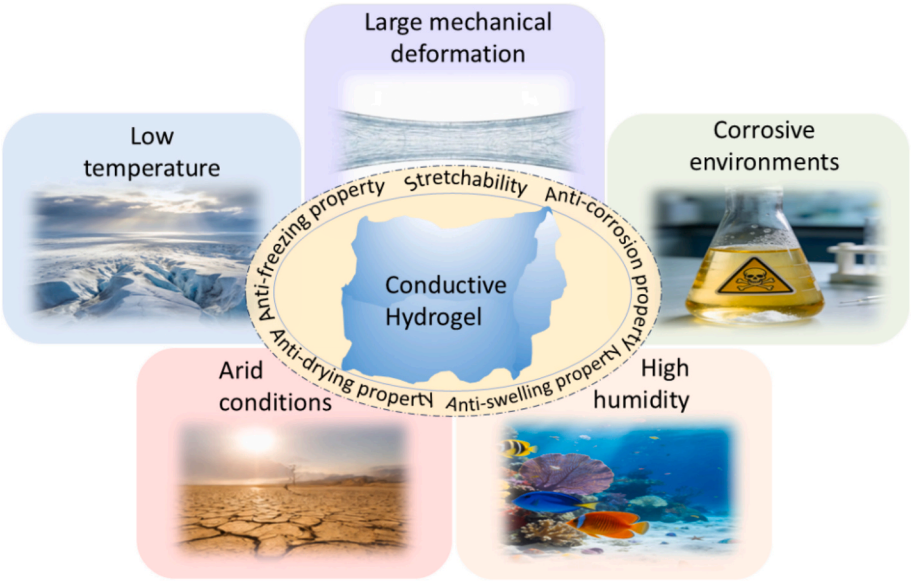


Fig. 2. Classification of five representative extreme environments and corresponding adaptive properties of conductive hydrogel sensors, including anti-freezing, anti-drying, anti-swelling, anti-corrosion, and stretchability.

Natural conductive hydrogels use polymers obtained from natural sources as the matrix. Common examples include gelatin, chitosan, alginate, and cellulose. Related studies have applied their composites with conductive fillers in the sensing field, for instance, Zhao et al. reported a self-healing poly(N-vinylpyrrolidone) (PVP)/gallic-acid composite hydrogel for wearable sensing [55]. Synthetic conductive hydrogels use chemically synthesized polymers as the matrix, with typical materials including polyacrylamide (PAM), polyacrylic acid (PAA), polyvinyl alcohol (PVA), and polyethylene glycol (PEG). Functional modification research on such synthetic polymers is extensive, for example, Sun et al. developed an ionically conductive hydrogel based on PAM and lithium chloride, which combines high stretchability, self-healing, and anti-freezing properties, making it suitable for flexible sensors [56].

In the context of performance optimization, combinations of natural and synthetic polymers can be used to form hybrid conductive hydrogels, balancing biocompatibility with mechanical and electrical properties. Hybrid conductive hydrogels combine natural and synthetic polymers to balance biocompatibility with mechanical and electrical performance. For example, Du et al. incorporated tannic acid (TA)-modified reduced graphene oxide (rGO) into a PVA network [57]. The conductive filler provided electrical pathways, whereas the PVA network supplied elasticity and mechanical support. The resulting hydrogel responded to both tensile strain and pressure, illustrating how matrix-filler integration can broaden the measurable deformation range. Nevertheless, filler dispersion and interfacial stability remain important constraints in such hybrid systems.

2.1.2. *Crosslinking of conductive hydrogels*

Hydrogels can be formed through two approaches, including physical crosslinking and chemical crosslinking. Physical crosslinking constructs a network through reversible non-covalent interactions, exemplified by hydrogen bonding [58], crystallization [59], protein interactions [60], ionic interactions [61,62], hydrophobic or hydrophilic interactions [63], and metal coordination [64]. Chemical crosslinking, in contrast, achieves crosslinking through the formation of stronger and more permanent covalent or ionic bonds between polymer chains. Mainstream methods include suspension polymerization [65], copolymerization [66], chemical reactions of relevant functional groups [67], and enzyme-mediated crosslinking [68], among others.

2.1.3. *Conductive components of conductive hydrogels*

Conductive hydrogels retain the hydrated polymer network of conventional hydrogels while incorporating ionic, electronic, or hybrid charge-transport pathways. These pathways arise from mobile ions, electronically conductive components, or their combination, whereas the polymer network provides mechanical compliance and water retention. According to the type of conductive component and the underlying conduction mechanism, conductive hydrogels can be classified into three categories: ionically conductive hydrogels, electronically conductive hydrogels, and hybrid conductive hydrogels. Among them, ionically conductive hydrogels rely on ion migration as the conduction mechanism, depending on ion transport channels and the aqueous environment within the hydrogel network. The introduced conductive components include acids such as hydrochloric acid (HCl) [69], sulfuric acid (H_2SO_4) [70], and phytic acid (PA) [71]. For the metal salts, including lithium chloride (LiCl) [72], sodium chloride (NaCl) [73], and calcium chloride ($CaCl_2$) [74], as well as ionic liquids such as 1-ethyl-3-methylimidazolium chloride ([EMIM]Cl) [75]. As we all know, charge conduction is achieved through the migration of ions within the hydrogel network. Electronically conductive hydrogels, in contrast, rely on electronic transport, depending on mechanisms such as electron tunneling and contact effects. The introduced conductive components mainly include metal nanomaterials [76,77], carbon-based materials [78,79], and conductive polymers [80,81]. Electrons are transported through pathways formed by these conductive components to generate electric current, and the conductivity is determined by the spatial distribution and arrangement of the conductive materials. Hybrid conductive hydrogels incorporate both ionic and electronic conductive components, thereby constructing dual ionic and electronic conduction pathways. This enables the integration of flexibility of ionic conduction with the high charge transport efficiency of electronic conduction.

Although the carrier type differs among ionic, electronic, and hybrid conductive hydrogels, bulk electrical conductivity is evaluated using the same geometry-corrected relationship:

$$\sigma = \frac{L}{RA} \tag{1}$$

Where σ is the electrical conductivity (S m^{-1}), L is the distance between the electrodes (m), R is the measured bulk resistance (Ω), and A is the effective cross-sectional area (m^2). The A descriptor enables comparison of charge-transport capability after accounting for specimen geometry,

which is a material parameter rather than an independent stimulus-to-signal conversion mechanism. Together, polymer sources, crosslinking modes, and conductive components determine the network architecture, charge-carrier pathways, and environmental stability of conductive hydrogels. These structural features provide the material basis for the stimulus-to-signal transduction mechanisms.

2.2. Transduction mechanisms under external stimuli and service environments

The electrical response of a conductive hydrogel has many determinants, such as the stimulus, the network, the transport pathway, and the electrode. Ionic, electronic, and hybrid conduction describe the identity and migration route of charge carriers. Transduction describes a conversion process. It explains how various stimuli are turned into electrical signals. These stimuli include mechanical load, temperature, water activity, and chemical composition. The following discussion therefore combines the physical origin of each pathway with the quantitative transfer metric appropriate to the corresponding external stimulus or service environment.

2.2.1. Mechanical deformation

Stretching, compression, bending, and pressure modify both the macroscopic geometry and the internal conductive pathways of a hydrogel. In ionically conductive hydrogels, deformation changes the dimensions and tortuosity of hydrated channels and can alter ion-polymer interactions and ionic mobility. In electronically conductive and hybrid hydrogels, deformation additionally changes contact, separation, and tunneling among conductive components. Under an applied electrical bias, these coupled effects are recorded as a normalized resistance change, $\Delta R/R_0$. The geometric contribution to resistance is described by $R = \rho L/A$, where tensile deformation generally increases the conductive-path length L and decreases the cross-sectional area A, whereas compression produces the opposite geometric tendency. In a conductive hydrogel, however, the resistivity ρ is itself strain dependent because the polymer network, mobile-ion environment, conductive-filler contacts, and hydrogel–electrode interface evolve during loading (Fig. 3a). The measured resistance is therefore a combined geometric and microstructural response rather than a purely dimensional effect, as expressed in Eq. (2):

$$R = \rho \frac{L}{A} \tag{2}$$

where R is the resistance (Ω), ρ is the resistivity (Ω m), L is the effective conductive-path length (m), and A is the effective cross-sectional area (m^2).

For strain-controlled measurements, electromechanical sensitivity is commonly quantified by the gauge factor (GF), as defined in Eq. (3):

$$GF = \frac{\Delta R}{R_0 \varepsilon} \tag{3}$$

where $\Delta R = R - R_0$, R_0 is the resistance in the undeformed state, and $\varepsilon = (L - L_0)/L_0$ is the applied tensile strain. GF is dimensionless and should be reported together with the corresponding strain interval. When the response is nonlinear, segmental GF values or the local slope $d(\Delta R/R_0)/d\varepsilon$ provide a more accurate description than a single value over the full deformation range. The PAM/mucin/TA/LiCl hydrogel shown in Fig. 3b illustrates the ionic form of this mechanism. The hydrated polymer network provides continuous ion-transport channels, while deformation changes channel geometry and the local environment of the mobile ions. Consequently, mechanical deformation is converted into a reproducible resistance response through the evolution of the ion-conduction pathway.

In addition to the resistance-based transduction described above, ionically conductive hydrogels can convert mechanical stimuli into electrical signals via piezoionic transduction. Mechanical loading of an ionically conductive hydrogel generates a pressure and deformation field within the hydrated network. Because cations and anions differ in

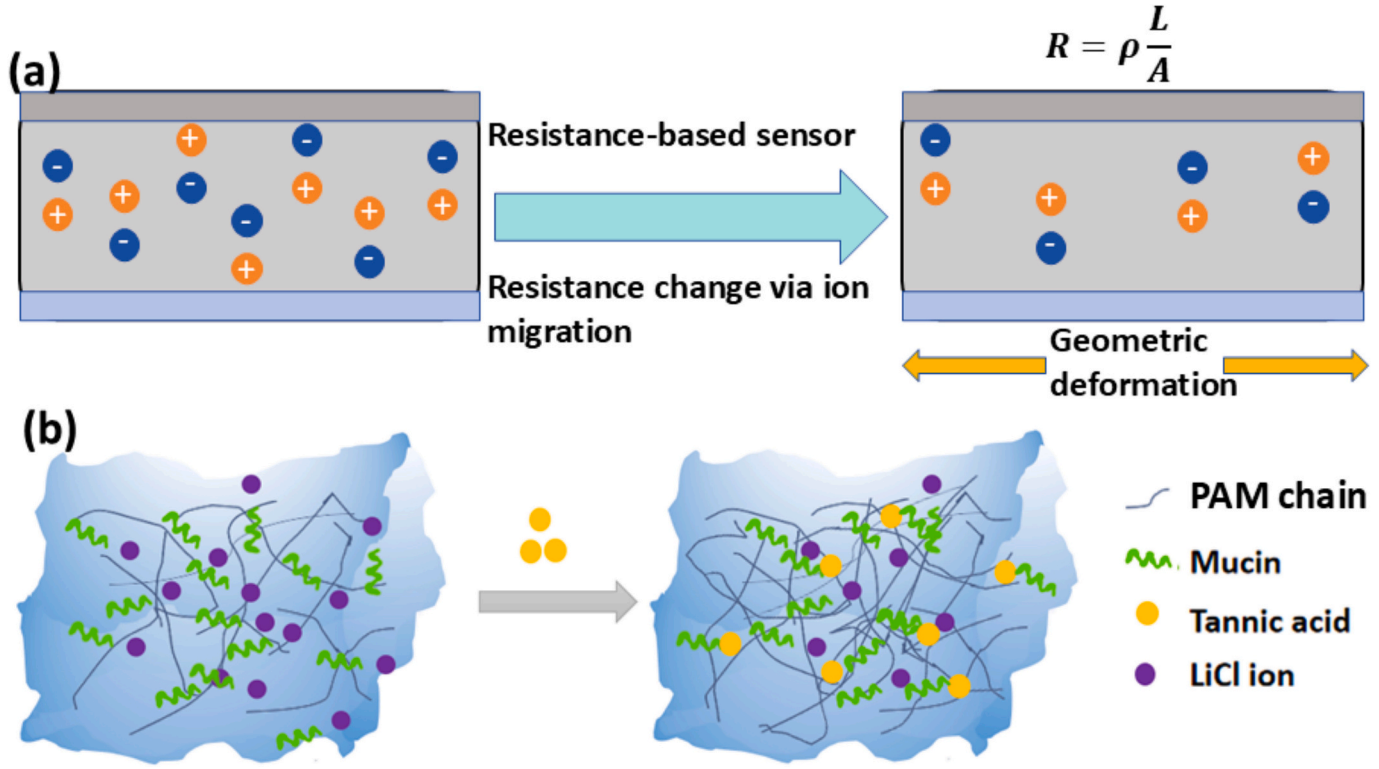


Fig. 3. Resistance-based transduction in conductive hydrogels. (a) Deformation-induced changes in specimen geometry and conductive pathways; (b) PAM/mucin/TA/LiCl hydrogel network illustrating regulation of hydrated ion-transport channels.

hydrated size, effective mobility, and affinity for the polymer chains and electrode interfaces, their fluxes are generally unequal. The resulting transient concentration polarization and interfacial charge separation produces an open-circuit voltage or short-circuit current (Fig. 4) [82]. This self-generated electrical output does not require external bias. Its amplitude and polarity are controlled by the mobility contrast between the ions, ion concentration, network permeability, specimen thickness, loading rate, and electrode configuration. After unloading, diffusion relaxes the ion-concentration and interfacial-charge gradients, leading to signal decay and, in some systems, a brief reverse peak. Because increasing salt concentration can simultaneously enhance ionic conductivity and strengthen electrostatic screening, conductivity and piezoionic voltage do not necessarily vary in parallel.

For pressure-controlled measurements, the voltage response can be compared quantitatively using the piezoionic voltage sensitivity defined in Eq. (4) ;

$$S_{PI} = \frac{\Delta V}{\Delta P} \tag{4}$$

where S_{PI} is the piezoionic voltage sensitivity (mV kPa^{-1}), ΔV is the change in open-circuit voltage (mV), and ΔP is the applied pressure interval (kPa). For a nonlinear response, the differential sensitivity dV/dP should be reported over the relevant pressure range. Meaningful comparison additionally requires consistent reporting of loading rate, specimen thickness, ion composition, and electrode configuration because these parameters govern ion-redistribution kinetics.

The origin of the piezoionic signal differs from intrinsic piezoelectricity. Piezoionic hydrogels generate electrical output through the redistribution of mobile ions, whereas intrinsic piezoelectric materials generate bound polarization charge through strain-induced changes in a non-centrosymmetric or explicitly piezoelectric phase. For comparison, the fluorinated polyimide nanofiber aerogel reported by Zhong et al. represents the latter process [83], its electrical output originates from solid-state polarization rather than ion migration within a hydrated conductive network.

2.2.2. Temperature variation

When the sensing element undergoes an approximately uniform temperature change, temperature modifies ion dissociation and mobility, polymer-segment dynamics, the state of water, and the contact or tunneling probability between electronically conductive components. These changes produce a temperature-dependent resistance $R(T)$, which is measured using an external circuit (Fig. 5a). The direction of the response is material dependent: increasing temperature often promotes ion motion, whereas thermoresponsive network contraction, dehydration, phase transition, or disruption of conductive contacts may instead increase resistance. Over a specified temperature interval, the normalized response is quantified by the temperature coefficient of resistance, α_T, as expressed in Eq. (5):

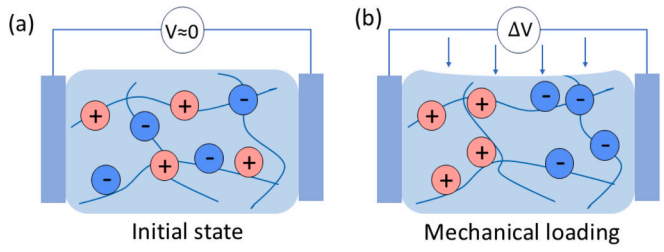


Fig. 4. Piezoionic transduction in an ionically conductive hydrogel. (a) Mobile cations and anions are approximately balanced in the unloaded state. (b) Mechanical loading induces unequal ion redistribution and interfacial charge separation, producing a voltage output (ΔV).

$$\alpha_T = \frac{\Delta R}{R_0 \Delta T_u} \tag{5}$$

where α_T is the temperature coefficient of resistance (K^{-1}), $\Delta R = R(T) - R_o$, R_o is the resistance at the reference temperature T_o, and $\Delta T_u = T - T_o$ is the approximately uniform change in device temperature. A positive α_T denotes an increase in resistance with temperature, whereas a negative value denotes a decrease. For a nonlinear $R(T)$ relationship, the local coefficient $\alpha_T\ (T) = (1/R)(dR/dT)$ should be reported as a function of temperature.

In contrast to strain-induced resistive and piezoionic responses under mechanical stimuli, conductive hydrogels can also convert thermal gradients into electrical signals via ionic thermoelectric transduction. A spatial temperature gradient provides a distinct thermodynamic driving force. Cations and anions with different heats of transport and thermodiffusive mobilities redistribute along the gradient, and the resulting charge separation generates an open-circuit voltage without an external bias (Fig. 5b). This Soret-driven contribution may coexist with a thermogalvanic potential when reversible redox couples are present. The ionic Seebeck coefficient, S_i, is defined as the open-circuit voltage generated per unit end-to-end temperature difference, as expressed in below Equation:

$$S_i = \frac{\Delta V_{OC}}{\Delta T_g} \tag{6}$$

where S_i is the ionic Seebeck coefficient (mV K^{-1}), ΔV_{oc} is the open-circuit voltage difference across the hydrogel (mV), and $\Delta T_g = T_h - T_c$ is the spatial temperature difference between the hot and cold ends (K). The sign of S_i follows the specified voltage and temperature directions. Ji et al. developed an MXene/PVA ionic thermoelectric hydrogel in which Cu^{2+} and Cl^- served as thermodiffusive carriers, producing a thermopower of −3.13 mV K^{-1} under an applied temperature gradient [84]. When the device temperature is spatially uniform, ΔTg approaches zero and the thermoelectric voltage vanishes; the remaining temperature response is then governed by $R(T)$.

2.2.3. Humidity variation and water exposure

Water activity is a central state variable that couples hydrogel structure to charge transport. During drying, the fraction of mobile water decreases, ion dissociation and mobility are restricted, and the polymer network contracts. The resistance of an ionically conductive hydrogel therefore generally increases after substantial water loss. In electronic and hybrid systems, network contraction can shorten the separation between conductive components and temporarily improve percolation, but excessive shrinkage may fracture conductive pathways or damage the hydrogel-electrode interface. The competition among these processes can produce nonlinear or even nonmonotonic electrical responses to decreasing humidity. Under high humidity or immersion, water sorption expands the network and changes channel dimensions, carrier concentration, ion-polymer association, and the spacing between electronically conductive components. Contact with an external liquid can additionally induce ion exchange, salt leaching, and interfacial delamination. Reversible coupling between water uptake and electrical resistance provides the basis for humidity or water sensing, whereas uncontrolled exchange produces baseline drift in sensors designed to measure other stimuli. Water-retaining coatings and hydrophobic encapsulation reduce fluctuations in internal water activity [85–87], while oriented or metal-coordinated networks restrict swelling-induced dimensional and conductive-path changes during immersion [87–89].

2.2.4. Chemical and corrosive media

Chemical media regulate conductive-hydrogel signals by changing both the carrier environment and the material interfaces. Variations in pH alter protonation and deprotonation of ionizable groups; dissolved salts modify ionic strength, activity coefficients, and ion partitioning;

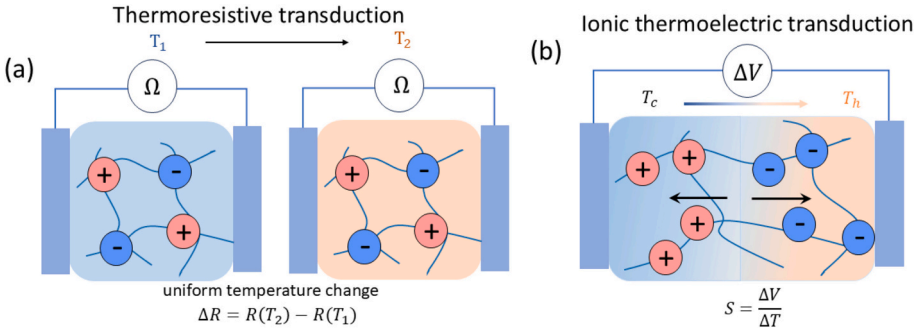


Fig. 5. Temperature-dependent transduction pathways in conductive hydrogels. (a) An approximately uniform temperature change modifies carrier transport and network state, producing a resistance response measured by an external circuit. (b) An end-to-end temperature gradient drives unequal ion thermodiffusion and generates an open-circuit voltage (ΔV).

and organic solvents change dielectric properties, polymer solvation, and network dimensions. Specific ions or biomolecules may also participate in complexation, competitive adsorption, or redox reactions. When these interactions are reversible and coupled to a selective recognition element, they can be transduced into an analyte-dependent resistance, potential, or impedance signal. Without molecular or interfacial selectivity, the same processes appear primarily as cross-sensitivity and baseline drift.

Prolonged exposure to corrosive media can further induce polymer-chain hydrolysis, loss of ionic species or conductive fillers, oxidation of electronic conductors, electrode corrosion, and interfacial debonding, thereby converting a reversible signal perturbation into irreversible performance decay. The extracellular-matrix-mimicking hydrogel evaluated in a moist, dynamic oral environment [90] and the PAHCT hydrogel tested in seawater, pH 3–11 media, and organic solvents [91] illustrate the need to stabilize the polymer network, conductive phase, and electrode interface simultaneously in chemically complex service environments.

2.2.5. *Coupled stimuli and signal interpretation*

Extreme service environments rarely contain a single independent variable. A resistance signal measured during mechanical deformation may simultaneously include contributions from specimen geometry, carrier mobility, water-induced swelling or shrinkage, conductive-filler contact, and electrode impedance. Similarly, a measured voltage may contain piezoionic, ionic thermoelectric, thermogalvanic, or electrode-polarization contributions when mechanical loading, temperature gradients, and chemical exchange coexist. The observed signal is therefore a composite transfer function of the stimulus history and the evolving material state.

Mechanistic attribution requires controlled variation of one environmental factor at a time, characterization of the spatial temperature field, comparison of biased resistance measurements with open-circuit voltage measurements, and evaluation of loading-rate, hysteresis, recovery, and baseline drift. GF, S_{pi}, α_t, and S_i quantify different stimulus-to-signal transfer functions and therefore cannot be ranked on a common numerical scale. Cross-sensitivity matrices or multichannel readouts are particularly valuable when several environmental variables coexist. Maintaining a stable and calibratable transfer function under such coupled exposure is central to the design of anti-freezing, anti-drying, anti-swelling, anti-corrosion, and highly deformable conductive-hydrogel sensors. Accordingly, reliable sensing under extreme environments requires both an identifiable transduction pathway and a material network capable of preserving that pathway during thermal, humidity/water, chemical, and mechanical exposure. Therefore, we discuss preparation strategies and adaptive properties that stabilize the hydrated polymer network, charge transport, and the hydrogel-electrode interface.

3. Preparation strategies and desired properties of conductive hydrogels

3.1. *Preparation strategies of conductive hydrogels*

Conventional hydrogel preparation primarily focuses on the formation of a 3D polymer network without considering the design of conductive pathways. In contrast, the preparation of conductive hydrogels requires coordinated control of electrical and mechanical properties between electrical and mechanical properties. To construct an electronically conductive network, electronically conductive hydrogels need strategies such as pre-assembly, in situ polymerization, and interface guiding to enable nanoscale conductive fillers to build a continuous 3D conductive pathway that adapts to deformation within the hydrogel matrix, avoiding rigid aggregation of the fillers. Ionically conductive hydrogels, on the other hand, require modulation of polymer chain hydrophilicity, crosslinking density, and microporous structure to construct hydrated channels that facilitate the rapid migration of ions such as Na^+ and Cl^-. Following the structured construction strategy for ionically conductive networks, many studies have optimized ion transport efficiency through hydrogen bond regulation and porous structure design. For example, Fu et al. developed a poly(vinylidene fluoride) (PVDF)-containing porous conductive hydrogel sponge with a multiscale architecture for discriminable multimodal sensing and gesture recognition [92] (Fig. 6a). To address the mutual constraints between mechanical and electrical properties of conductive hydrogels, current research often employs multi-network composite designs to achieve decoupled regulation of these properties. With a functional layered design, the robust polymer network undertakes mechanical deformation and external loads, and the independent conductive network sustains stable conductive paths. In addition, the conductive network is engineered into flexible microstructures including wavy and spring-like configurations. The relative slip between the two network phases during deformation realizes the decoupling and synergistic optimization of mechanical and electrical performance. Based on this preparation concept of electromechanical synergy and structural decoupling, some studies have optimized the network integration mode through molecular grafting modification, breaking through the performance bottlenecks of traditional materials. For instance, DeVolder et al. prepared a sodium alginate-g-pyrrole conductive hydrogel through grafting and crosslinking modification with pyrrole monomers (Fig. 6b). By optimizing the network composite mode at the molecular structure level, they overcame the trade-off between mechanical and electrical properties typically observed in conventional ionic hydrogels, achieving simultaneous improvement in mechanical performance and electrical conductivity through tuning the degree of monomer substitution [93]. In addition to basic network construction and electromechanical regulation, enhancing the environmental stability of the conductive network through formulation modification and structural optimization is also a

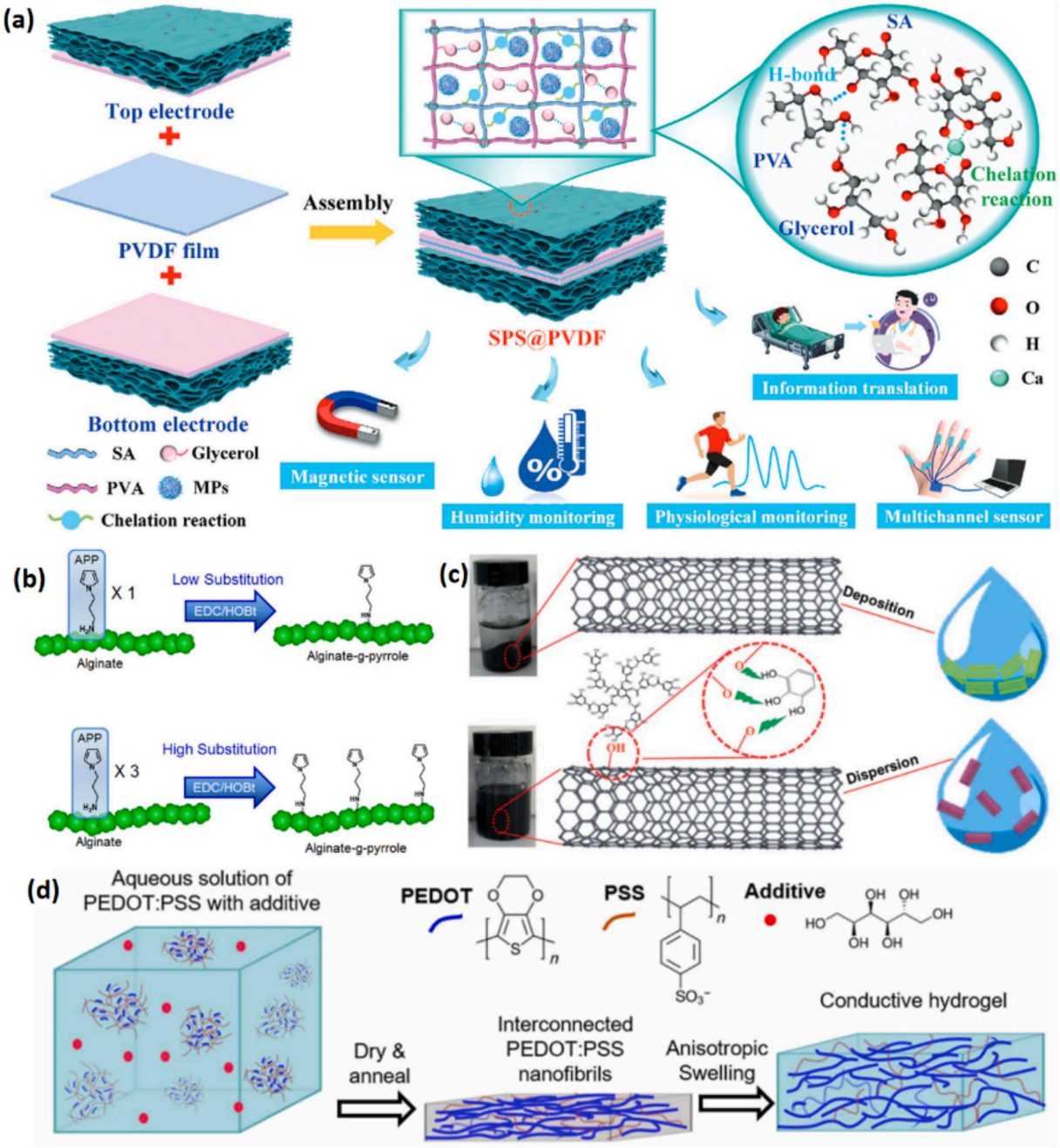


Fig. 6. Typical preparation strategies of conductive hydrogels: (a) Fabrication of the PVDF-containing porous conductive hydrogel sponge and its multimodal sensing applications. Reproduced with permission [92]. Copyright 2024, Wiley-VCH. (b) Schematic illustration of the network construction principle of sodium alginate-g-pyrrole. Reproduced under a Creative Commons Attribution (CC BY) license [93]. (c) Schematic illustration of the mechanism by which TA promotes the dispersion of carbon nanotubes in solution. Reproduced with permission [94]. Copyright 2020, The Royal Society of Chemistry. (d) Preparation of dry films using PEDOT:PSS aqueous solution with D-sorbitol, followed by conversion of the dry films into stable conductive hydrogels through anisotropic swelling. Reproduced under a Creative Commons Attribution (CC BY) license [95].

key strategy in the preparation of conductive hydrogels. Introducing water-retaining additives such as glycerol and sorbitol, or constructing hydrophobic coatings, can mitigate dehydration of hydrogels. Optimizing the crosslinked network can enhance anti-swelling and dimensional stability, while interface modification can effectively reduce electrode resistance. For example, He et al. prepared a TCGP conductive hydrogel using a glycerol-water binary system combined with tannic acid-modified carbon nanotube doping (Fig. 6c). Through composition regulation and dense crosslinked structure design, they simultaneously achieved structural characteristics including anti-freezing, moisture retention, anti-swelling, and low interfacial impedance, significantly improving the network stability in complex environments [94]. Furthermore, green additive modification and process optimization are also important preparation methods for enhancing the comprehensive stability of hydrogels. For instance, Rahman et al. used non-toxic D-sorbitol as a modifying additive, combined with micromolding processing to optimize the micro-network structure of poly(3,4-ethylenedioxythiophene):poly(styrene sulfonate) (PEDOT:PSS) hydrogels (Fig. 6d). Through green component modification and structural optimization, they effectively enhanced the electromechanical structural stability of the hydrogel under extreme environments and improved its interfacial conductivity, achieving simple preparation of

highly stable conductive hydrogels [95].

3.2. Desired properties of conductive hydrogels

Through rational material design, conductive hydrogels can be endowed with multiple adaptive properties, including anti-freezing, anti-drying, anti-swelling, anti-corrosion, and stretchability, enabling stable sensing under complex environments. However, improving one environmental adaptability often introduces compromises in other properties, such as mechanical robustness, electrical conductivity, sensing sensitivity, and long-term stability. Therefore, understanding the advantages, limitations, applicable conditions, and intrinsic trade-offs of different adaptive strategies is essential for the rational design of conductive hydrogel sensors.

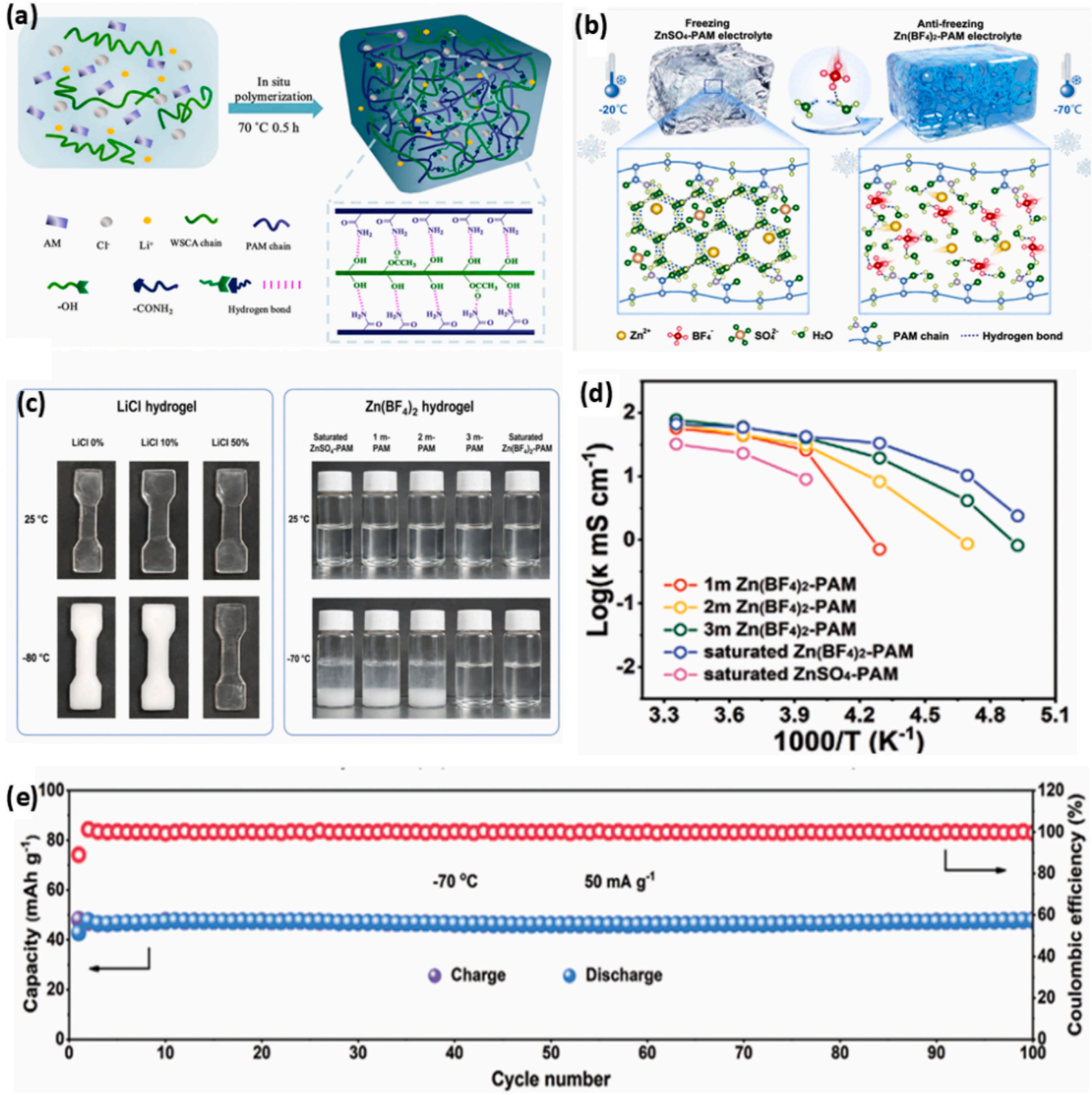


Fig. 7. Salt-regulation strategies for improving the anti-freezing performance of conductive hydrogels. (a) Schematic illustration of LiCl-based double-network hydrogel formation through polymer network reinforcement and salt-induced hydration regulation. Reproduced with permission [96]. Copyright 2022, Elsevier Ltd. (b) Morphological evolution of LiCl-containing hydrogel under subzero temperatures, demonstrating structural preservation. Reproduced with permission [97]. Copyright 2023, Wiley-VCH. (c) Anti-freezing mechanism of $Zn(BF_4)_2$-PAM hydrogel based on ion–water interactions and hydrogen-bond regulation. Reproduced with permission [96]. Copyright 2022, Elsevier Ltd. Reproduced with permission [97]. Copyright 2023, Wiley-VCH. (d) Visual comparison of $Zn(BF_4)_2$-PAM hydrogel stability at room temperature and − 70 °C. (e) Long-term cycling performance of the $Zn(BF_4)_2$-PAM hydrogel-based zinc-ion battery at −70 °C. Reproduced with permission [97]. Copyright 2023, Wiley-VCH.

3.2.1. Anti-freezing property

Low-temperature environments pose a serious challenge to the practical application of conductive hydrogel-based soft electronic devices. Due to their high water content, hydrogels are prone to freezing below the freezing point, resulting in loss of flexibility and elasticity, while the ion transport pathways are blocked, leading to a near-complete loss of their conductive function. Therefore, endowing hydrogels with anti-freezing capability is key to expanding their applications in frigid regions, high-altitude areas, or deep-water environments.

The anti-freezing property of hydrogels essentially depends on the state of water within them. Water molecules can be classified into three types: free water, intermediate water, and bound water. The amount of free water is a key factor determining the freezing behavior of hydrogels. The essence of freezing is the ordered arrangement of water molecules through hydrogen bonding to form ice crystals. Therefore, a general strategy for anti-freezing design is to introduce specific components into the hydrogel system to effectively disrupt the regular hydrogen bonding network among water molecules, thereby inhibiting the nucleation and growth of ice crystals.

Modulating water states within polymer networks has become a mainstream strategy for improving anti-freezing performance, mainly through the introduction of inorganic salts, zwitterionic compounds, and polyhydric organic solvents. However, achieving anti-freezing capability while maintaining mechanical integrity, electrical conductivity, and sensing stability remains challenging. Among these approaches, inorganic salt regulation is widely adopted because hydrated ions can reduce free water content, disrupt water–water hydrogen bonding, and suppress ice crystal formation. Zhang et al. constructed a PAM/water-soluble cellulose acetate double-network hydrogel based on a synergistic strategy of "polymer network reinforcement and high-concentration salt ions" and introduced high-concentration LiCl [96]. Due to the strong hydration effects of Li^+ and Cl^-, ice crystal formation was effectively suppressed, while hydrogen-bond interactions between the double networks further stabilized the polymer structure (Fig. 7a). When the LiCl mass fraction was no less than 30%, the hydrogel remained soft and elastic at −80 °C (Fig. 7b), with a tensile strength of 341 kPa and toughness of 1.2 MJ m^{-3}, demonstrating effective preservation of mechanical integrity under subzero conditions [96]. Compared with LiCl-based double-network systems, Shi et al. introduced zinc tetrafluoroborate ($Zn(BF_4)_2$) into a PAM network to achieve enhanced low-temperature stability through stronger ion–water interactions and disruption of the hydrogen-bonding network (Fig. 7c) [97]. When the $Zn(BF_4)_2$ concentration reached ≥3 M, the hydrogel maintained flexibility at −70 °C (Fig. 7d). Furthermore, the corresponding zinc-ion battery exhibited stable cycling performance at −70 °C, maintaining nearly 100% coulombic efficiency after 100 cycles (Fig. 7e), indicating its potential for low-temperature energy-related applications [97].

Biomass reinforcement can complement, but does not replace, water-state regulation. Zhu et al. used 2,2,6,6-tetramethylpiperidine-1-oxyl (TEMPO)-oxidized cellulose nanofibers (TOCNs) and tannic-acid-mediated interactions in microfluidically spun conductive hydrogel fibers, coupling a reinforced hydrogen-bond network with a continuous sensing pathway and demonstrating mechanically robust strain sensing, including low-temperature operation [98]. The scientific contribution is the fiber-scale integration of renewable reinforcement, processability, and signal transduction, representing an emerging direction from single-function cryoprotection toward multifunctional environmental adaptation. From the perspective of structure–property relationships, both LiCl and $Zn(BF_4)_2$ regulate the water state through ion hydration and disruption of water–water hydrogen bonding, thereby suppressing ice crystallization and improving low-temperature stability. However, these two strategies exhibit different advantages and limitations. The LiCl-containing double-network strategy combines anti-freezing capability with mechanical reinforcement by integrating salt-induced hydration and polymer network stabilization, whereas $Zn(BF_4)_2$-based systems provide stronger freezing resistance through enhanced ion–water interactions but require relatively high salt concentrations. Excessive salt incorporation may disturb polymer-network interactions, reduce mechanical adaptability, and compromise long-term stability. Therefore, salt-based anti-freezing design involves a trade-off among freezing resistance, mechanical integrity, ionic conductivity, and additive loading. Insufficient ion–water interactions may lead to ice formation, whereas excessive salt regulation may induce structural instability [96,97].

Recent biomass-reinforced strategies further indicate that anti-freezing conductive hydrogels are evolving from single-component cryoprotection toward integrated regulation of water states, polymer architecture, and conductive pathways. Future designs should focus on balancing freezing resistance, mechanical adaptability, and sensing reliability under complex low-temperature environments.

3.2.2. Anti-drying property

Owing to their high water content, hydrogels are highly susceptible to dehydration in arid conditions, leading to volume shrinkage and structural deformation that compromise the mechanical stability and electrical reliability of conductive hydrogel-based soft electronic devices. Therefore, improving anti-drying capability is essential for maintaining long-term sensing performance under arid conditions. The studies discussed here mainly employ two surface-protection strategies for improving the anti-drying property of conductive hydrogels: hydrophobic elastomer encapsulation and hydrophilic water-retaining coatings, which prevent dehydration through physical isolation and interfacial water regulation, respectively [85,86]. Yuan et al. adopted an in situ elastomer encapsulation strategy by selecting butyl acrylate and hexafluorobutyl methacrylate as soft and hard functional monomers, respectively. Through surface-confined copolymerization, a dense hydrophobic elastic coating was generated in situ on the hydrogel surface (Fig. 8a) [86]. This protective layer not only suppresses internal water evaporation but also resists swelling induced by external media, thereby improving the structural stability of the hydrogel during prolonged environmental exposure. At 25 °C and 30% RH, the unencapsulated PAM hydrogel retained only 20.90 ± 0.02% of its weight after 2 days of storage, whereas the encapsulated PAM-P(B_2F_1) composite hydrogel maintained a weight retention of 71.90 ± 2.55% after 7 days, with no obvious volume shrinkage and sustained softness and elasticity (Fig. 8b) [86].

In contrast to hydrophobic encapsulation, hydrophilic water-retaining coatings suppress dehydration by strengthening water–surface interactions rather than isolating the hydrogel from the external environment. For example, Gao et al. developed a quenched dual-hydrophilic coating strategy inspired by natural hydrophilic macromolecular structures [85]. In this design, sulfonate groups were first enriched on the hydrogel surface, and cationic gelatin was immobilized through electrostatic interactions to form a surface film. Glycerol was then introduced to construct a dual-hydrophilic structure, followed by quenching treatment in glycerol at −20 °C to induce the sol-gel transition of gelatin and form a dense hydrophilic barrier. At 25 °C and 40% RH, the unmodified hydrogel lost more than 70% of its water on the first day and retained only about 20% of its weight after 5 days, whereas the quenched PAM-P5G30Q hydrogel achieved a weight retention of 72.5% ± 2% after 5 days (Fig. 8b). Representative photographs further confirmed that the protected hydrogel exhibited much less volume shrinkage and better morphological stability during dehydration (Fig. 8c) [85].

A recent hydrogel-elastomer hybrid illustrates how biomass can support interfacial environmental protection rather than serve merely as a sustainability label. Lu et al. incorporated carboxymethyl cellulose (CMC) into a LiCl-containing PAM ionic hydrogel and encapsulated it with polydimethylsiloxane (PDMS) [87]. The hybrid retained more than 98% of its water over long-term storage, reached approximately 91.2% transmittance, and enabled mechanical–thermal sensing from −20 to

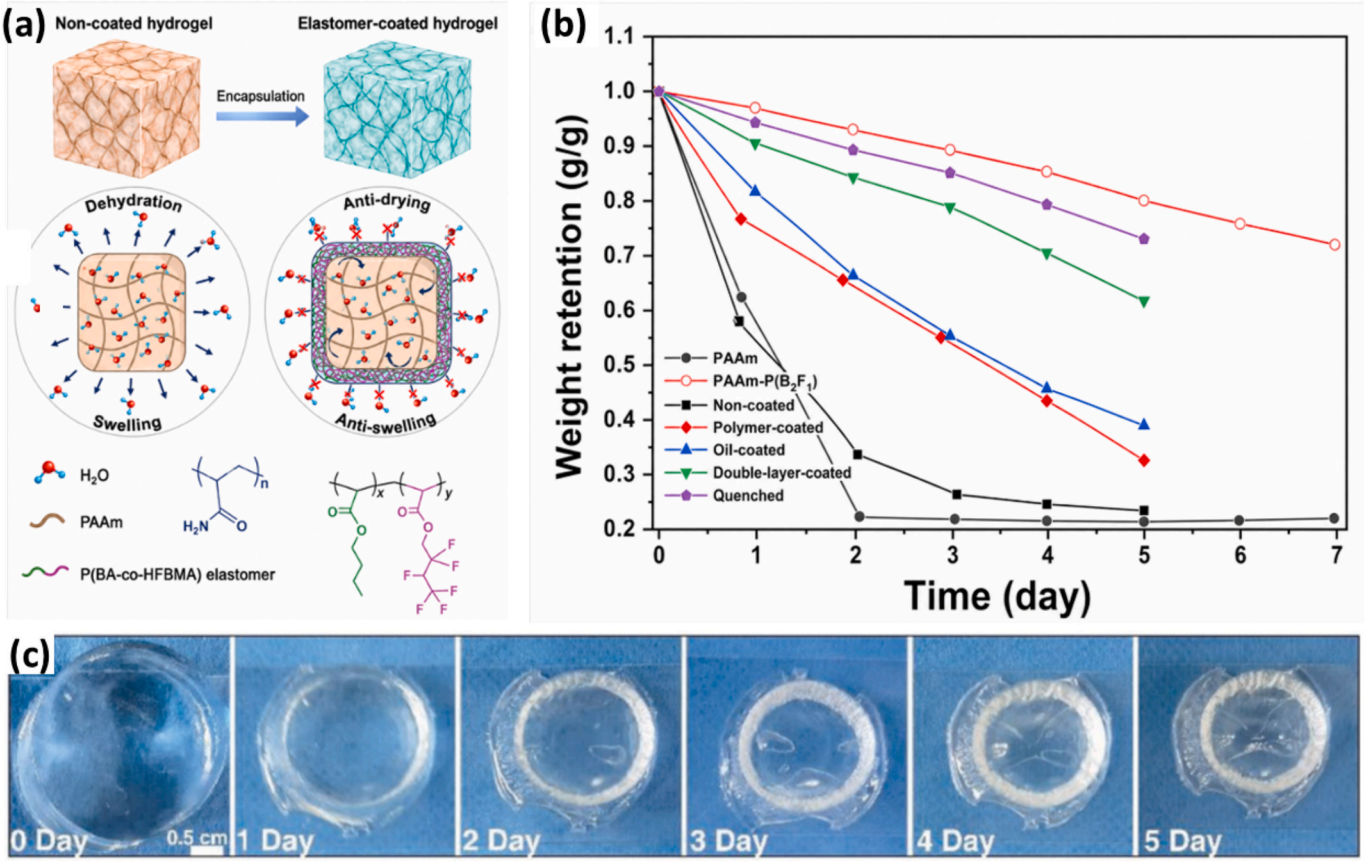


Fig. 8. Anti-drying performance of conductive hydrogels. (a) Schematic of elastomer-coated hydrogels for protection against drying and swelling. (b) Weight retention of PAM and PAM-P(B_2F_1) hydrogels during an air-drying test at 25 °C and 30% RH, together with a comparison of surface-protection strategies during dehydration at 25 °C and 40% RH. Reproduced with permission [86]. Copyright 2024, Wiley-VCH. (c) Photographs showing morphological changes during dehydration. Reproduced with permission [85]. Copyright 2023, Wiley-VCH.

60 °C (temperature coefficient of resistance (TCR) ≈ −1.1% $°C^{-1}$; GF ≈ 3.8), together with underwater information transmission. CMC contributes network reinforcement and water management, while the elastomer provides the dominant vapor/liquid barrier. This division of roles is important: the result demonstrates system-level environmental tolerance, not intrinsic non-drying behavior of an unencapsulated biomass hydrogel.

These two surface-protection strategies provide different advantages. Hydrophobic elastomer encapsulation offers a stronger barrier against water evaporation and simultaneously suppresses external-medium-induced swelling, making it suitable for prolonged exposure to arid conditions; however, the added barrier may increase interfacial complexity and restrict mass transport. By contrast, hydrophilic coatings retain water through strong interfacial interactions and better preserve hydrogel-like surface characteristics, but their protective effect may be more sensitive to coating integrity and ambient humidity. Therefore, anti-drying design requires balancing water retention, interfacial compatibility, permeability, and long-term coating stability; biomass-derived hydrophilic networks can construct adaptive hydration environments maintaining both moisture stability and sensing functionality beyond conventional barrier-based protection, yet barrier cracking or coating delamination will trigger rapid water loss, network shrinkage and sensing drift [85,86], so future anti-drying conductive hydrogels should balance water retention, interfacial durability and functional stability instead of merely pursuing dehydration suppression.

3.2.3. *Anti-swelling property*

Excessive water absorption during prolonged aqueous exposure is a major challenge for conductive hydrogels used in underwater and physiological sensing. Uncontrolled swelling expands the polymer network, compromises mechanical and electrical stability, and may induce dimensional mismatch with surrounding tissues. Panda et al. combined pre-stretching-induced chain orientation with Fe^{3+}-mediated dual crosslinking to construct a dense and oriented network [88]. The pre-oriented polymer chains were locked through hydrophobic association and metal–ligand coordination, thereby restricting water penetration (Fig. 9a). This hydrogel exhibited only a slight volume change after being immersed in water for 2 days, showing far superior anti-swelling stability compared to untreated samples. Among them, the sample with 200% pre-stretching showed significantly improved mechanical properties, with a tensile strength of 2.48 MPa, a fracture strain of 268%, and a toughness of 3.85 MJ m^{-3}, which are approximately 9 times, 6.7 times, and 55 times those of the non-pre-stretched sample, respectively (Fig. 9b **and** Fig. 9c). Field-emission scanning electron microscopy (FESEM) and small-angle X-ray scattering (SAXS) confirmed the formation and locking of the oriented network. The reversible resistance response during underwater strain sensing further demonstrated that network orientation can simultaneously improve dimensional stability and sensing reliability.

Unlike the pre-stretching strategy, which relies on macroscopic chain orientation and subsequent structural locking, Huang et al. regulated polymer–water interactions at the molecular level by grafting poly (copper-arylacetylide) onto a PVA network [89]. The grafted component disrupted hydrogen bonding between PVA and water while forming a dense metal-coordination network that limited water penetration (Fig. 9d). The resulting PVA-CAA4% hydrogel exhibited an equilibrium swelling ratio of approximately 0% after 8 days of immersion, compared with 55% for pure PVA (Fig. 9e). After 20 days, it retained 88% of its

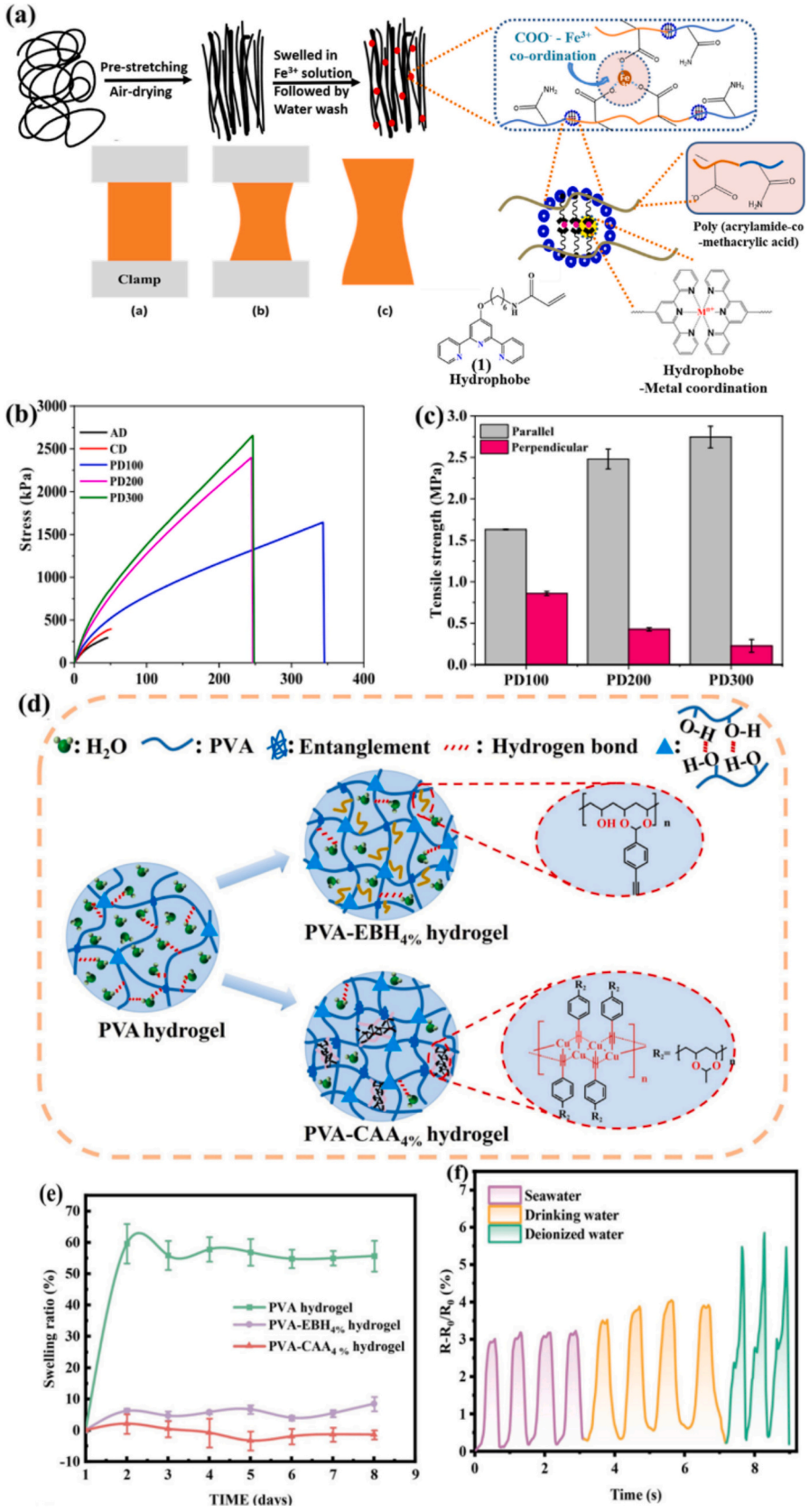


Fig. 9. Anti-swelling mechanisms and performance of conductive hydrogels. (a) Pre-stretching-induced orientation and Fe^{3+} coordination. (b) Stress-strain curves and (c) tensile strengths of PD100–PD300 hydrogels. Reproduced with permission [88]. Copyright 2025, American Chemical Society. (d) anti-swelling networks of PVA-EBH4% and PVA-CAA4% hydrogels. (e) Swelling ratios after immersion in deionized water, and (f) resistance responses during finger bending in seawater, drinking water, and deionized water. Reproduced with permission [89]. Copyright 2024, The Royal Society of Chemistry.

initial toughness and remained structurally stable in different aqueous environments (Fig. 9f). These results indicate that molecular regulation can provide persistent dimensional stability, although dense coordination may restrict polymer-chain mobility. Li et al. combined ice-templated anisotropy with Hofmeister-effect salting-out to construct an oriented PVA/carboxylated carbon nanotube (CNT) hydrogel [99]. The reported swelling ratio was approximately 0.8%, and dimensional/electrical stability was maintained for one month in aqueous media; the aligned hydrogel also reached about 3 MPa tensile strength along the orientation direction. This work is scientifically significant because the same structural treatment improves load transfer and restricts water uptake, showing that anti-swelling design can be integrated with mechanical reinforcement and long-term signal stability rather than treated as an isolated dimensional-control problem.

These strategies suppress swelling at different structural levels. Pre-stretching followed by dual crosslinking provides pronounced mechanical reinforcement and is advantageous for underwater strain sensing, but the resulting anisotropy may produce direction-dependent properties and requires an additional mechanical processing step. Metal-coordination network design directly weakens polymer-water interactions and provides persistent dimensional stability, although excessive coordination may reduce chain mobility and mechanical compliance. By comparison, ice-templated anisotropic networks combined with salting-out offer very low swelling and long-term underwater durability, but their directional architecture and multistep processing may limit applications requiring isotropic deformation or simplified fabrication. Therefore, anti-swelling design requires balancing dimensional stability, mechanical isotropy, deformability, processing complexity, and sensing response. Incomplete structural locking, coordination-bond disruption, or deterioration of the oriented network may restore water penetration, resulting in network expansion and signal drift.

3.2.4. *Anti-corrosion property*

Conductive hydrogel devices exposed to corrosive environments face coupled risks of chemical degradation, excessive swelling, component leaching, and loss of interfacial stability. To maintain long-term structural and functional stability in corrosive environments, current designs primarily aim to reduce medium penetration, suppress swelling-induced damage, and stabilize the polymer network. A representative strategy is the construction of chemically stable double networks that integrate a rigid protective framework with a deformable supporting network. Using this concept, a biomimetic extracellular-matrix hydrogel (EMH) was developed for moist and dynamic oral environments (Fig. 10a) [90]. In this design, genipin-crosslinked chitosan (G-CS) formed a rigid fibrous framework, followed by PAM network incorporation to construct a double-network structure. The reinforced framework improved chemical stability and restricted medium penetration during prolonged aqueous exposure. After immersion in phosphate-buffered saline (PBS) simulating the oral environment, EMH maintained structural integrity without obvious degradation or component loss (Fig. 10b). The highly crosslinked CG-32 EMH exhibited a swelling ratio of only 29%, while

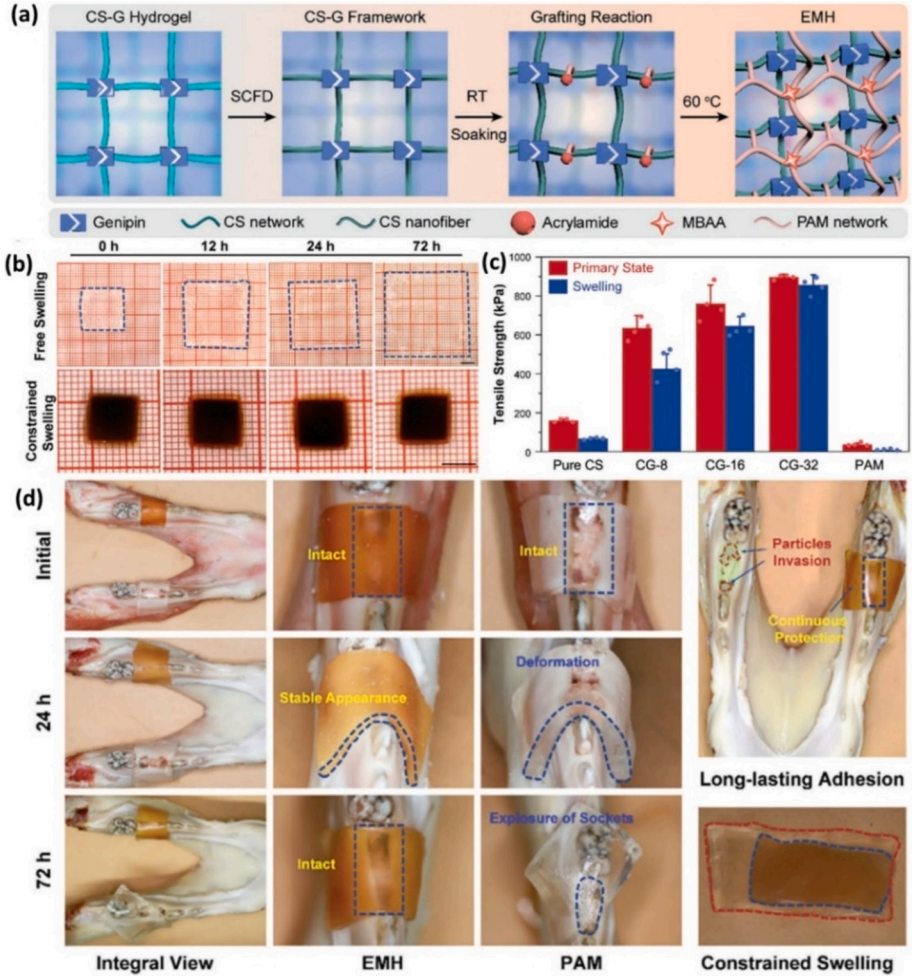


Fig. 10. Anti-corrosion performance of conductive hydrogels. (a) Construction of the G-CS/PAM double-network EMH. (b) Volume change of EMH and PAM hydrogels after PBS immersion. (c) Tensile strength before and after equilibrium swelling. (d) Morphological stability of EMH and PAM dressings during dynamic exposure in simulated physiological environments. Reproduced with permission [90]. Copyright 2022, Wiley-VCH.

maintaining a tensile strength of approximately 800 kPa after swelling. In contrast, pure PAM hydrogel showed severe swelling and significant mechanical deterioration (Fig. 10c). Antibacterial tests showed that the drug-loaded EMH achieved killing rates of 89.2% against *Staphylococcus aureus* and 98.7% against *Porphyromonas gingivalis*, two common oral pathogenic bacteria, thereby providing additional protection against bacterial contamination in the oral environment. In a dynamic corrosion simulation test (Fig. 10d), EMH showed no damage or detachment after 3 days in a flow system containing simulated food particles, whereas pure PAM hydrogel became deformed due to corrosion and swelling after 24 h and completely detached from the wound surface after 72 h. This double-network strategy integrates low swelling, mechanical reinforcement, and resistance to dynamic fluid exposure, making it suitable for long-term protection in moist physiological environments. However, its performance depends strongly on the integrity of the rigid framework and covalent interfacial connections. Excessive crosslinking may increase stiffness and reduce interfacial adaptability, whereas insufficient grafting may promote medium penetration and component loss. Moreover, the demonstrated corrosion resistance is mainly validated in a simulated oral environment and may not directly translate to strongly acidic, alkaline, or high-salinity conditions. Therefore, anti-corrosion design requires balancing chemical stability, mechanical compliance, and interfacial durability, with framework fracture, interfacial debonding, and progressive swelling representing potential failure pathways [90].

3.2.5. *Stretchability*

Stretchability is a key mechanical property for conductive hydrogels used in harsh environments, including repeated deformation in wearable electronics and dynamic motion in biointegrated devices. However, highly stretchable networks often suffer from insufficient mechanical strength and structural instability due to reduced crosslinking density. Therefore, current strategies mainly focus on introducing effective energy dissipation mechanisms while maintaining conductive pathways and network integrity. Constructing double-network (DN) structures is a widely adopted strategy for improving hydrogel stretchability. In these systems, the sacrificial first network dissipates mechanical energy through reversible fracture, while the second network maintains structural integrity during deformation. Li et al. developed an ultra-stretchable PAM-DVB-Li hydrogel through the construction of

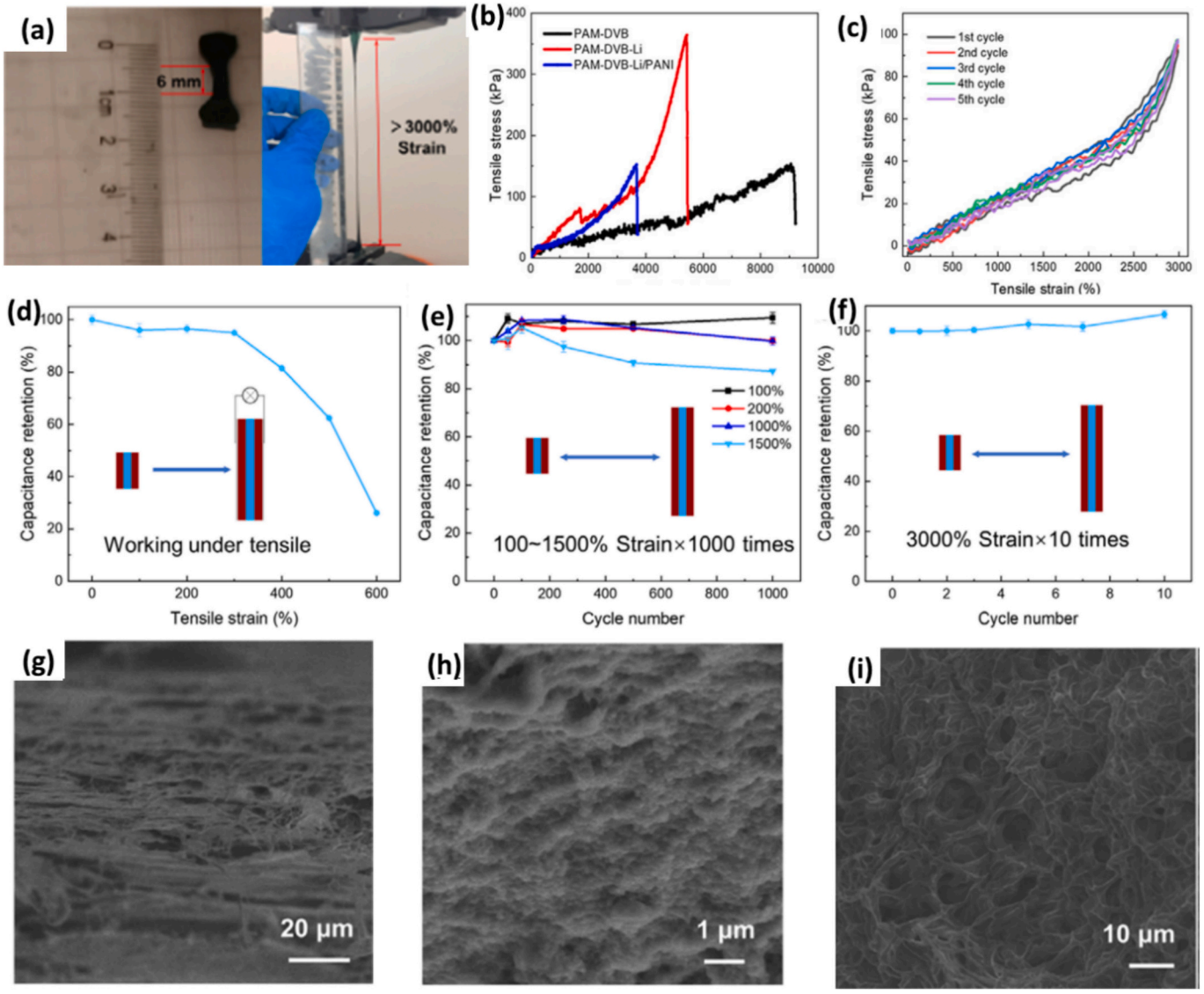


Fig. 11. Stretchability and electrochemical stability of conductive hydrogels. (a) PAM-DVB-Li/PANI integrated supercapacitor under large deformation. (b) Tensile behavior of PAM-DVB-based hydrogels and integrated devices. (c-f) Mechanical cycling stability and capacitance retention under different stretching conditions. (g-i) Microstructural evolution of hydrogel and PANI layers during deformation. Reprinted under a Creative Commons Attribution (CC BY) license [100].

hydrophobic divinylbenzene (DVB) crosslinking nodes, hydrophilic polymer networks, and γ-ray-induced polymerization [100]. In this design, hydrophobic DVB nodes reinforced the PAM network, while Li_2SO_4 contributed to toughness enhancement and ionic conductivity through ionic interactions. The resulting PAM-DVB-Li/polyaniline (PANI) integrated supercapacitor maintained structural integrity under 3000% strain without obvious fracture (Fig. 11a).

Systematic mechanical characterization demonstrated that the PAM-DVB-Li hydrogel achieved an elongation at break of 5627 ± 241% and a tensile strength of 334 ± 27 kPa, while the integrated device retained high deformability and electrochemical stability under repeated stretching (Fig. 11b-f). Microstructural observations further confirmed that the hydrogel network underwent reversible morphological adjustment rather than catastrophic fracture during deformation, supporting the long-term stability of the integrated device (Fig. 11g-i). Although DN strategies effectively improve stretchability, excessive dependence on sacrificial networks may introduce trade-offs between extensibility, recovery behavior, and structural complexity. Moreover, highly stretchable hydrogels designed for mechanical durability may still face challenges in maintaining stable conductivity under extreme deformation, long-term fatigue loading, and environmental fluctuations. Therefore, future stretchable conductive hydrogels should focus on the coordinated optimization of energy dissipation, conductive network reconstruction, interfacial stability, and sensing accuracy rather than maximizing elongation alone.

The above strategy demonstrates that stretchability can be improved by constructing energy-dissipative networks and maintaining conductive pathway integrity under deformation. However, different reinforcement approaches inevitably involve trade-offs among mechanical robustness, conductivity retention, sensing sensitivity, and fabrication complexity. Double-network structures provide effective toughness enhancement through sacrificial bond breaking, but excessive network reinforcement may restrict chain mobility and reduce responsiveness. Dynamic or reversible networks can improve recovery capability, whereas their long-term stability under repeated deformation remains challenging. Therefore, the design of stretchable conductive hydrogels should focus not only on achieving large deformation but also on maintaining signal reliability and structural durability during cyclic operation. Large elongation is not sufficient evidence of durability, while the crack growth, hysteresis, conductive-pathway reconstruction, and baseline drift must also be evaluated. In a mussel-inspired TOCN-supported graphene hydrogel, Ma et al. reported 0–600% strain sensing, a GF of 12, and 95.7% self-recovery within 60 min, linking reversible catechol/coordination interactions to fatigue resistance [101]. Lignosulfonate was used by Ma et al. as a renewable shell and compatibilizer for liquid-metal nanodroplets in PVA; the resulting composite reached 1.60 MPa tensile stress and 4.87 S m^{-1} conductivity while suppressing droplet leakage and phase separation [102]. Sang et al. used TOCNs to stabilize a polydopamine-modified black-phosphorus conductive network, obtaining strain and pressure sensing (GF 6.0; pressure sensitivity 0.13 kPa^{-1}) together with near-infrared (NIR) response [103]. These studies show three distinct biomass roles-load-bearing reinforcement, filler compatibilization, and multifunctional dispersion, rather than one generic green additive effect. To further compare the adaptive strategies discussed above, Table 1 summarizes their advantages, limitations, applicable environments, and typical failure modes.

As summarized in Table 1, each adaptive strategy improves resistance against a specific environmental stress by regulating water state, network structure, or conductive pathways; however, no single strategy can simultaneously maximize all performance parameters. These intrinsic trade-offs highlight the necessity of multi-property synergistic design, where complementary strategies are integrated to achieve balanced environmental adaptability and sensing reliability.

3.2.6. *Principles of multi-property synergistic design*

Practical conductive hydrogel systems rarely rely on a single adaptive strategy, because improving one environmental tolerance often introduces trade-offs in other performance parameters. For example, increasing cryoprotective additives can effectively inhibit ice formation but may reduce mechanical strength through plasticization, whereas excessive network reinforcement can improve structural stability but restrict flexibility and sensing sensitivity. Therefore, reliable operation under multiple extreme environments requires the synergistic integration of functional components, hierarchical network structures, and interface engineering rather than independent optimization of individual properties. In this review, “biomass-based” refers to materials that physically contain a biomass-derived substance, such as cellulose, nanocellulose, lignosulfonate, or wood, which performs an identifiable function. “Bioinspired” denotes a structural or chemical concept drawn from biology, such as mussel adhesion or tissue anisotropy. Notably, a bioinspired hydrogel may remain entirely synthetic despite its biological inspiration.

One effective strategy for achieving multiple functionalities is component-level regulation, in which different components are introduced to provide complementary functions. He et al. incorporated TA-coated carbon nanotubes (TA-CNTs) into a PVA-glycerol hydrogel

Table 1
Comparative analysis of adaptive strategies for conductive hydrogels under extreme environments: advantages, limitations, applicable scenarios, and failure modes.

Adaptive strategy	Typical design strategy	Advantages	Limitations	Applicable environments	Typical failure modes
Anti-freezing	Cryoprotectants, hydrated salts, ionic liquids, and water-state regulation	Suppresses ice nucleation, maintains ion mobility, and preserves flexibility under subzero conditions	Excessive additives may cause plasticization, ion leakage, and reduced mechanical strength or biocompatibility	Subzero and cryogenic environments (typically below 0 °C)	Ice crystal formation, reduced ion transport, and freezing-induced loss of sensing performance
Anti-drying	Polyols, hygroscopic additives, water-retaining agents, and surface encapsulation	Suppresses water evaporation and maintains hydrogel softness during dehydration	May reduce breathability, increase diffusion resistance, or slow sensing response	Arid and low-humidity environments (typically RH <30%)	Water loss, network shrinkage, embrittlement, and signal instability
Anti-swelling	Dense crosslinking, hydrophobic modification, network orientation, and metal coordination	Improves dimensional stability and maintains sensing accuracy in aqueous environments	Excessive network restriction may reduce elasticity and sensitivity	High-humidity environments and prolonged aqueous exposure	Network expansion, dimensional instability, and sensing signal deviation
Anti-corrosion	Protective coatings, dynamic networks, double-network structures, and chemical stabilization	Improves resistance against acidic, alkaline, saline, and organic media	Enhanced chemical stability may compromise flexibility or processing complexity	Corrosive environments including acidic or alkaline solutions, high ionic-strength media, and organic solvents	Chemical bond cleavage, network degradation, swelling, and conductivity deterioration
Stretchability	Double-network structures, sliding networks, dynamic crosslinking, and nanocomposite reinforcement	Provides large deformation tolerance, energy dissipation, and mechanical durability	Complex fabrication, hysteresis, and possible reduction in sensitivity and response linearity	Large-strain and dynamic deformation scenarios	Network fracture, irreversible conductive pathway disruption, and sensing drift

system [94]. In this design, glycerol regulated the water state to improve anti-freezing and moisture-retention capabilities, CNTs established conductive pathways, and hydrogen-bond interactions between TA and PVA enhanced mechanical stability. This multifunctional design enabled the simultaneous integration of environmental adaptability, electrical conductivity, and mechanical robustness, demonstrating the potential of rational component combination for multifunctional conductive hydrogels. Beyond component regulation, network engineering and conductive interface modulation provide additional approaches for balancing multiple properties. Rahman et al. developed a D-sorbitol-modified PEDOT:PSS hydrogel, where sorbitol-induced phase separation generated conductive nanofibrous structures while maintaining mechanical adaptability and environmental stability [95]. This strategy demonstrates that regulating conductive network formation and interfacial interactions can simultaneously improve electrical performance, mechanical adaptability, and long-term stability, although excessive structural modification may increase design complexity and require careful optimization for specific applications.

Two recent studies exemplify complementary routes to multi-property integration. Zheng et al. combined TOCN-supported graphene with a PAM/PAA/polydopamine double network and glycerol [104]. The organohydrogel retained function across −20 to 70 °C, achieved a GF of approximately 15, and combined adhesion and biocompatibility with motion sensing. Meanwhile, glycerol mitigated freezing and evaporation, while TOCNs provided reinforcement and dispersion of the conductive phase. In a cellulose-mediated liquid-metal composite, Ma et al. used the polysaccharide phase to stabilize the conductive filler and build adhesive mechanical-thermal multimodal sensing [105]. The latter broadens functionality, but quantitative comparison requires common thermal cycling, aging, and cross-sensitivity protocols. Together, these papers move beyond additive accumulation by assigning different components to separable environmental, interfacial, and transduction roles.

Bioinspired interfacial engineering provides a second, conceptually distinct route. Mussel-inspired catechol chemistry can improve wet adhesion and reversible energy dissipation, as illustrated by the TOCN/graphene system [101]. Because the biological inspiration lies in interfacial chemistry and TOCN supplies the biomass-derived phase, both descriptors are appropriate here. In other systems, however, only one may apply. Such interfaces should be evaluated by adhesion retention after defined immersion and by sensing drift during repeated attachment, rather than by initial lap-shear strength alone. Data-assisted optimization is promising for balancing multiple properties, but it should not be inferred from conventional compositional screening. The oxidation-resistant, self-healable PVA-catechol/MXene hydrogel reported by Chae et al. [106] is better interpreted as structure- and interface-guided materials design. Future machine-learning claims should disclose the dataset, descriptors, validation strategy, uncertainty, and prospective experimental confirmation. Without these elements, ‘AI-assisted’ wording overstates the evidence.

Overall, multi-property synergistic design represents a transition from single-function optimization toward integrated regulation of hydrogel components, network structures, and interfaces. However, increasing functional complexity also introduces challenges related to fabrication scalability, structural stability, component compatibility, and long-term reliability. Potential failure modes, including phase separation, network degradation, interface failure, and loss of conductive pathways, should therefore be carefully considered during multifunctional hydrogel design. Future development should focus on balancing environmental adaptability, mechanical robustness, electrical performance, and practical applicability rather than maximizing individual properties.

4. Applications of conductive hydrogels

For a visual overview of the principal design logic and performance differences of conductive hydrogels under various extreme environments, and to aid targeted material selection for subsequent applications, Table 2 summarizes the key information from representative studies in recent years. All data are derived from explicit content in the original references, focusing on protection strategies, core properties, and application suitability that are closely related to the original context.

Table 1 and Table 2 provide strategy-level and environment-level comparisons, respectively. Table 3 complements them with a study-level quantitative comparison of representative conductive hydrogel systems reported during the past five years. The requested fields are retained even when a study did not report a value; such entries are marked NR rather than estimated. Because GF is not applicable to every transduction mode, voltage, thermoelectric, or transistor-specific sensitivity is reported where appropriate.

Conductive hydrogels, leveraging their unique ionic conduction mechanism and flexible network structure, have demonstrated potential for sensing applications under various extreme environments, whereas conventional sensing materials often struggle to maintain stable performance under such harsh conditions. Conductive hydrogel-based sensing systems are often required to withstand harsh environmental challenges such as extreme temperature fluctuations, severe humidity variations, and corrosive solution attack. At the same time, they must endure large mechanical deformations and, even when physical damage occurs, rapidly restore sensing functionality through self-healing properties, ensuring stability and reliability during long-term use. To address these requirements, recent advances have gradually shifted conductive hydrogel-based sensing systems from single-environment tolerance toward multifunctional environmental adaptation. In particular, biomass-derived components and bioinspired molecular interactions have attracted increasing attention because they can provide renewable resources, improved biocompatibility, and dynamic interactions with polymer networks. By integrating biomass-based functional units with conductive networks and protective structures, emerging hydrogel sensors are capable of simultaneously addressing environmental stability, mechanical durability, and sensing reliability, providing new opportunities for wearable electronics, biomedical monitoring, and self-powered sensing platforms. In this section, we systematically review and discuss advanced sensing applications of conductive hydrogels designed for these extreme conditions.

4.1. Extreme temperature and humidity

Extreme temperature and humidity variations represent critical environmental challenges for conductive hydrogel-based sensing systems. Low temperatures induce ice crystallization, restrict ionic migration, and reduce mechanical flexibility, whereas dry environments accelerate water evaporation and lead to network shrinkage and signal instability. Conversely, excessive humidity or prolonged aqueous exposure may cause uncontrolled swelling, interfacial deterioration, and sensing deviation. Therefore, practical conductive hydrogel sensors require integrated regulation of water state, polymer network structure, and interface interactions to simultaneously maintain environmental stability and sensing reliability. Recent advances have shifted conductive hydrogel-based sensing systems from single-environment tolerance toward multifunctional environmental adaptation. Rather than simply incorporating antifreeze or water-retaining components, current strategies increasingly focus on constructing adaptive networks that dynamically respond to temperature and humidity fluctuations. Climate-resilient sensing requires in situ signal retention, not simply survival after storage. The MA-PR hydrogel maintained sensing after 30 days at −42 °C and sequential seawater exposure [107], while the penguin-skin-inspired PAP-MCP/APD system converted deformation into piezoionic output for rehabilitation monitoring at low temperature [108]. The PAOAM-PDO organohydrogel integrated freezing tolerance, water retention, strain sensing, and triboelectric energy generation

Table 2
Environment-specific protection strategies, core performance metrics, and application scenarios for conductive hydrogels.

Type of extreme environment	Core protection strategy	Core performance metrics	Suitable application scenarios
Low temperature (≤ − 20 °C)	High-concentration salt ions and polymer network reinforcement	Anti-freezing temperature:-40 ~ −80 °C Electrical conductivity:≥2.38 mS cm^{-1}	Motion monitoring in cold environments, low-temperature energy storage devices
Arid conditions (RH ≤ 30%)	In situ elastomer encapsulation and quenched dual-hydrophilic coating	Weight retention after 7 d:≥71% ; No obvious embrittlement	Wearable sensors for high-altitude or arid regions
High humidity or underwater	Pre-stretching orientation and metal coordination network	Swelling ratio:≤5.5% ; Underwater sensing stability time:≥ 7 d	Underwater motion monitoring, amphibious communication devices
Corrosive solutions (pH 2–12)	Double-network structure and interface modification	pH tolerance range:2–12 No degradation in seawater for 7 d	Marine operation equipment, implantable sensors
Large mechanical deformation (≥1000%)	Double network (DN) and dynamic crosslinking	Elongation at break:≥3500% Signal fidelity after 2000 cycles:≥87%	Flexible human–machine interaction, electrophysiological monitoring of dynamic tissues

Table 3
Quantitative comparison of representative conductive hydrogel sensing systems under extreme environments reported during the past five years.

Material/system	Operating condition	Electrical conductivity	GF/sensitivity	Stretchability	Cycling stability	Water-retention / aqueous-stability time	Ref.
PAAm-P(B_2F_1) hydrogel–elastomer composite	25 °C, 30% RH	NR	N/A	NR	NR	71.90 ± 2.55% mass retained after 7 d	[86]
Pre-stretched Fe^{3+}-coordinated anisotropic hydrogel	Water immersion for 2 d	NR	NR	268% fracture strain	Reversible underwater resistance response; cycle number NR	Only slight volume change after 2 d immersion	[88]
PVA-CAA4% hydrogel	Aqueous immersion, 8–20 d	NR	NR	341% elongation at break	Reversible finger-bending signals; cycle number NR	≈0% equilibrium swelling after 8 d; 88% toughness retained after 20 d	[89]
MA-PR hydrogel sensor	−42 °C for 30 d; seawater; 2.2 °C seawater	NR	2.29 (−42 °C); 5.94/2.37 (7/30 d seawater); 2.77 (2.2 °C)	Tested to 300% strain	NR	Functional sensing retained after 30 d air storage and 30 d seawater immersion	[107]
PAP-MCP/APD piezoionic hydrogel	−80 °C; ambient air for 7 d	NR	GF 9.1; 1495 mV maximum output	NR	NR	66.6% mass remaining after 7 d	[108]
PAOAM-PDO organohydrogel	−24 °C sensing; DSC: −60 to 20 °C	0.79 S m^{-1} at −24 °C; 1.13 S m^{-1} at room temperature	GF 7.05 at 233% strain	233% sensing strain	NR	>90% mass retained after 10 d at 25 °C, 60% RH	[109]
PAHCT hydrogel sensor	Seawater; pH 3–11; organic solvents	NR	NR	990% fracture strain	800 cycles at 100% strain	5.5% swelling after 48 h in seawater; chemical stability assessed for 7 d	[91]
THIN hydrogel–elastomer nanomembrane/OECT	Dynamic tissue; hydrated state	NR	N/A; OECT μC = 1034 F cm^{-1} V^{-1} s^{-1}	No cracking at 200% strain	≥30 d in vivo signal monitoring	N/A	[110]
PAPL hydrogel sensor/ electrode	Ambient; cyclic strain	NR	NR; detection limit 0.1% strain	1050% fracture strain	2000 cycles at 100% strain with no obvious drift	NR	[111]
CMC/LiCl hydrogel–PDMS hybrid	−20 to 60 °C; underwater	NR	GF ≈ 3.8; TCR ≈ −1.1% $°C^{-1}$	NR	100 loading–unloading cycles reported for fatigue evaluation	>98% water retained after 15 d drying in air	[87]
TOCN/graphene organohydrogel	−20 to 70°C	NR	GF ≈ 15	NR	NR	NR	[104]

Note. NR, not reported; N/A, not applicable to the stated transduction mode. GF, TCR, and OECT are defined at their first occurrence in the main text. Values are reported only under the stated test conditions and are not extrapolated across different transduction modes.

[109]. These examples represent different transduction modes and should not be ranked by a single sensitivity metric. Among recent biomass-based systems, the microfluidic TOCN fiber [98], the CMC/LiCl hydrogel–elastomer hybrid [87], and the TOCN/graphene organohydrogel [104] further show how renewable reinforcements can be combined with salts, glycerol, or encapsulation to retain conductive pathways across temperature and moisture stresses. For example, Bai et al. prepared an MA-PR conductive hydrogel utilizing the synergistic effect of a polyrotaxane sliding ring structure and multiple hydrogen bonds [107]. After being stored at an extreme low temperature of −42 °C for 30 days, this hydrogel still exhibited a GF of 2.29 and could stably monitor joint motion signals of fingers, wrists, and knees. After 30 days of storage in ambient air at room temperature, the GF remained at 3.46, with stable resistance change signal output (Fig. 12a-12f). In high-humidity and underwater extreme environments, this hydrogel retained swelling resistance: after immersion in seawater for 7 and 30 days, the GF values were 5.94 and 2.37, respectively, enabling accurate capture of finger and elbow joint movements underwater. In low-temperature seawater at 2.2 °C, the GF was 2.77, successfully achieving motion monitoring in winter swimming scenarios (Fig. 12g-

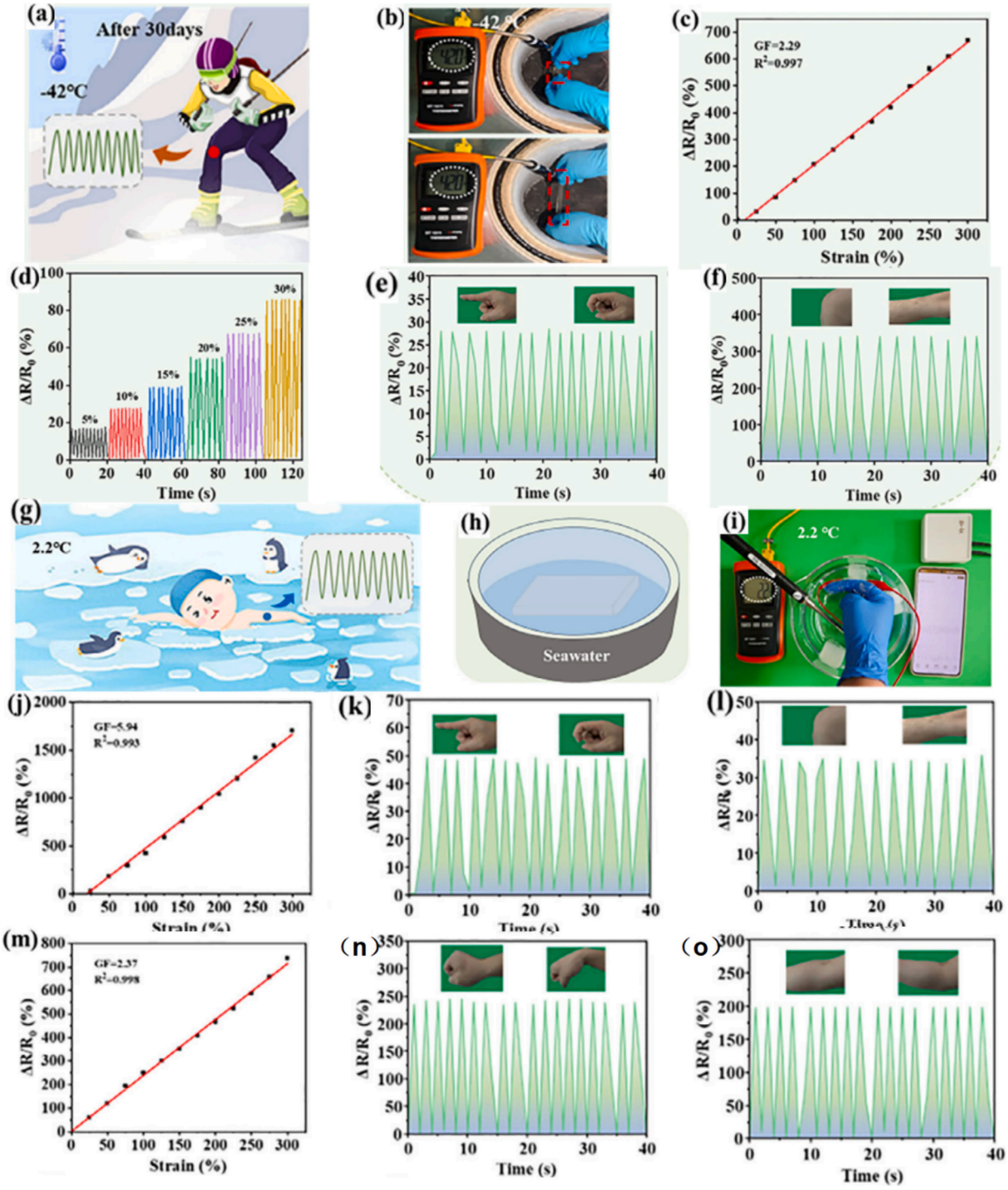


Fig. 12. Sensing performance of the MA-PR hydrogel after storage at −42 °C and seawater immersion. (a) Low-temperature sensing mechanism; (b) photograph of the test at −42 °C; (c,d) strain-dependent resistance responses; (e,f) finger- and knee-motion monitoring; (g-j) winter-swimming simulation and sensing after 7 days of seawater immersion; and (k-o) motion monitoring after 30 days of seawater immersion. Reproduced with permission [107]. Copyright 2025, Wiley-VCH.

12o).

In addition to being directly used for underwater motion monitoring, the sensing performance of conductive hydrogels under extreme environments can also be extended to the field of medical rehabilitation. Inspired by penguin skin, Zheng et al. prepared a PAP-MCP/APD conductive hydrogel with anti-freezing and anti-drying properties through a dual-layer coating composed of (3-aminopropyl)triethoxysilane (APTES) and perfluoropolyether (PFPE) combined with *N*,*N*-dimethylformamide as an antifreeze additive [108]. This hydrogel remained elastic at −80 °C, and differential scanning calorimetry (DSC) showed no ice crystal formation peak. After 7 days of storage in air at room temperature, the maximum water loss rate was only 33.4%, with a tensile strength of 1156 kPa and a compressive strength of 3.45 MPa. For piezoionic sensing, this hydrogel exhibited a response time of 0.4 s, a recovery time of 1.0 s, a GF as high as 9.1, a maximum output voltage of 1495 mV, and a power density of 3.4 mW m^{-2}. Owing to its stable output under extreme environments, this hydrogel was integrated into rehabilitation training sensing systems, including a grip training glove and a balance training insole, enabling accurate capture of pressure changes during hand grasping of different objects and plantar force distribution

(Fig. 13a,b). Even in an environment of −80 °C, this hydrogel maintained a stable piezoionic output (approximately 1000 mV) without freezing-induced embrittlement, enabling continuous motion sensing and data transmission in extremely cold environments (Fig. 13c,d).

In addition to scenario-specific sensing applications, the comprehensive performance of multifunctional conductive hydrogels under extreme environments can also be extended to self-powered sensing systems. For example, Zhao et al. prepared a PAOAM-PDO organohydrogel through a one-step free radical polymerization method using a PDO-water binary solvent system with oxidized sodium alginate, aminated gelatin, acrylic acid, and $AlCl_3$ as raw materials [109]. DSC measurements showed that this hydrogel exhibited no ice crystal formation peak in the range of −60 °C to 20 °C, remained flexible and conductive at −24 °C (conductivity of 0.79 S m^{-1}), and could serve as a skin barrier to prevent low-temperature frostbite. At room temperature, it achieved a GF of 7.05 at 233% strain, with a response time of 0.5 s and a recovery time of 1.2 s. It could accurately monitor large-scale motions such as wrist bending, finger flexion and extension, and knee movement, as well as subtle actions such as smiling and writing (Fig. 14a-d). The hydrogel also exhibited water-retention capability, retaining over 90% of its mass after a 10-day storage period at 25 °C and 60% RH, while remaining transparent and soft (Fig. 14e,f). Furthermore, PAOAM-PDO was assembled into a single-electrode mode triboelectric nanogenerator (TENG), achieving an open-circuit voltage of 350 V and a power density of 0.81 W m^{-2}, capable of lighting up 25 LEDs connected in series, demonstrating its potential for self-powered sensing systems.

Recently, biomass-based environment-adaptive conductive hydrogels have further broadened the application potential of flexible sensors by integrating renewable components with functional sensing architectures. CMC reinforces the ionic network, while PDMS offers the main dehydration barrier [87]. TOCNs stabilize the conductive phase and glycerol provides the principal freezing/drying resistance [104], with cellulose mediating liquid-metal dispersion and interfacial adhesion for multimodal mechanical–thermal sensing [105].

Overall, applications of conductive hydrogels under extreme temperature and humidity conditions are gradually evolving from short-term demonstration of environmental resistance toward practical wearable and intelligent sensing systems. Future progress requires simultaneous consideration of environmental adaptability, user comfort, device lifetime, scalable fabrication, and integration with real-world electronic platforms.

4.2. Corrosive solutions and large mechanical deformation

Corrosive solutions, such as seawater and industrial acidic or alkaline liquids, pose severe environmental challenges for sensing applications of conductive hydrogels. Conventional conductive hydrogels in such environments are prone to swelling, degradation, or loss of electrical conductivity due to ion exchange and network disruption, making it difficult to maintain stable sensing functionality. For example, Wu et al. prepared a PAHCT conductive hydrogel using an ultraviolet (UV)-curable dense double-network strategy, with acrylic acid, hydroxyethyl methacrylate, quaternized chitosan, and TA as a raw material [91]. This hydrogel exhibited an equilibrium swelling ratio of only 5.5% in seawater after 48 h of immersion, far superior to the control hydrogel, which showed a swelling ratio of 317% and complete rupture failure. It achieved a tensile fracture strain of 990% and a fracture strength of 96 kPa, and maintained stable electrical signal output after 800 cyclic stretching cycles at 100% strain. The strain sensor based on this hydrogel could accurately monitor flexion and extension movements of joints such as fingers, wrists, and elbows underwater. By utilizing different bending angles (30° for dot and 90° for dash), it achieved underwater communication using Morse code, enabling real-time transmission of distress signals such as “SOS” and “help me” (Fig. 15a-c). This hydrogel can effectively resist the erosion of seawater salt ions, maintain long-term sensing performance, and meet the sensing demands in fields such as marine operations and underwater rescue.

In practical applications such as wearable monitoring and flexible human–machine interaction, conductive hydrogel-based sensor devices often need to withstand large mechanical deformations and even physical damage. Conventional conductive hydrogels are prone to loss of sensing functionality due to network structure fracture and disruption of conductive pathways, severely affecting their service life and reliability. To address this issue, conductive hydrogel sensing technologies with self-healing properties have been extensively investigated. By introducing dynamic crosslinking interactions or optimizing network structure design, these hydrogels can autonomously repair structural defects and reconstruct conductive pathways after large deformation or physical damage, rapidly restoring sensing performance and ensuring long-term stable operation.

In addition to corrosive environments, dynamic tissues in living organisms (such as beating hearts and contracting muscles) impose higher demands on stable sensing under large deformation. For example, Jung et al. developed a THIN hydrogel-elastomer conductive nanomembrane with a total thickness of only 350 nm [110]. Its dry-state modulus was 1.35 GPa, which decreased to 0.035 GPa after hydration, and its bending stiffness decreased from 0.16 to 9.08 × 10^{-5} GPa μm^4, achieving an instantaneous phase transition from rigid free-standing to soft conformable states. This nanomembrane exhibited no crack generation under 200% tensile strain, maintaining intact crystalline alignment and charge transport pathways. When assembled into an organic electrochemical transistor (OECT), it achieved a μC value (mobility × volumetric capacitance) as high as 1034 F cm^{-1} V^{-1} s^{-1} and an interfacial impedance of only 138.4 Ω at 1 kHz. The THIN-based OECT devices operated stably on dynamic tissues such as rat myocardium, tibialis anterior muscle, and cerebral cortex, accurately capturing electrograms (EGM), electromyograms (EMG), and electrocorticograms (ECoG), with no signal drift during long-term monitoring, meeting the high-precision sensing demands of biomedical dynamic tissues (Fig. 16a-e).

In addition to in vivo dynamic tissue monitoring in biomedical applications, conductive hydrogels with low hysteresis and cyclic stability are also suitable for long-term stable acquisition of daily human activities and physiological signals. For example, Lv et al. prepared a PAPL conductive hydrogel through a strategy of regulating polymer chain entanglement and constructing hydrogen bond-assisted hydrophobic aggregates [111]. This hydrogel achieved a tensile strength of 310 kPa, a fracture strain of 1050%, and a hysteresis ratio below 5.4% at 800% strain, demonstrating low hysteresis at large strain. As a strain sensor, it exhibited a detection limit as low as 0.1% tensile strain and a response time of only approximately 16.6 ms. After 2000 stretching cycles at 100% strain, the signal showed no obvious drift. It could accurately capture both subtle and large-scale human motions such as fist clenching, eye movement, breathing, and pulse (Fig. 17a-d). Furthermore, the PAPL hydrogel can serve as a dry electrode for physiological electrical signal acquisition. The signal-to-noise ratios of the recorded ECG, electroencephalogram (EEG), electrooculogram (EOG), and EMG were superior to those of commercial Ag/AgCl electrodes. After 1000 stretching cycles, it still maintained signal fidelity, meeting the requirements for rehabilitation training monitoring and clinical physiological signal acquisition (Fig. 17e,f).

Beyond wearable and bioelectronic monitoring, recent biomass-based hydrogels extend the application space toward self-sensing actuation. A TOCN-mediated bilayer system integrates thermoresponsive deformation with electrical feedback [112], while a related TOCN gradient system enables NIR-driven deformation and self-sensing [78]. Delignified-wood architectures, in turn, provide rapid programmable bending and anisotropic reinforcement [113]. A multi-stimuli wood/Fe_3O_4/liquid-metal/TOCN-poly(N-isopropylacrylamide) (PNIPAM) actuator further combines thermal, NIR, and magnetic control with intrinsic electrical readout [114]. These studies support an emerging sensing–actuation direction, although the recent review by Li et al. emphasizes that resistance readout should not yet be equated with

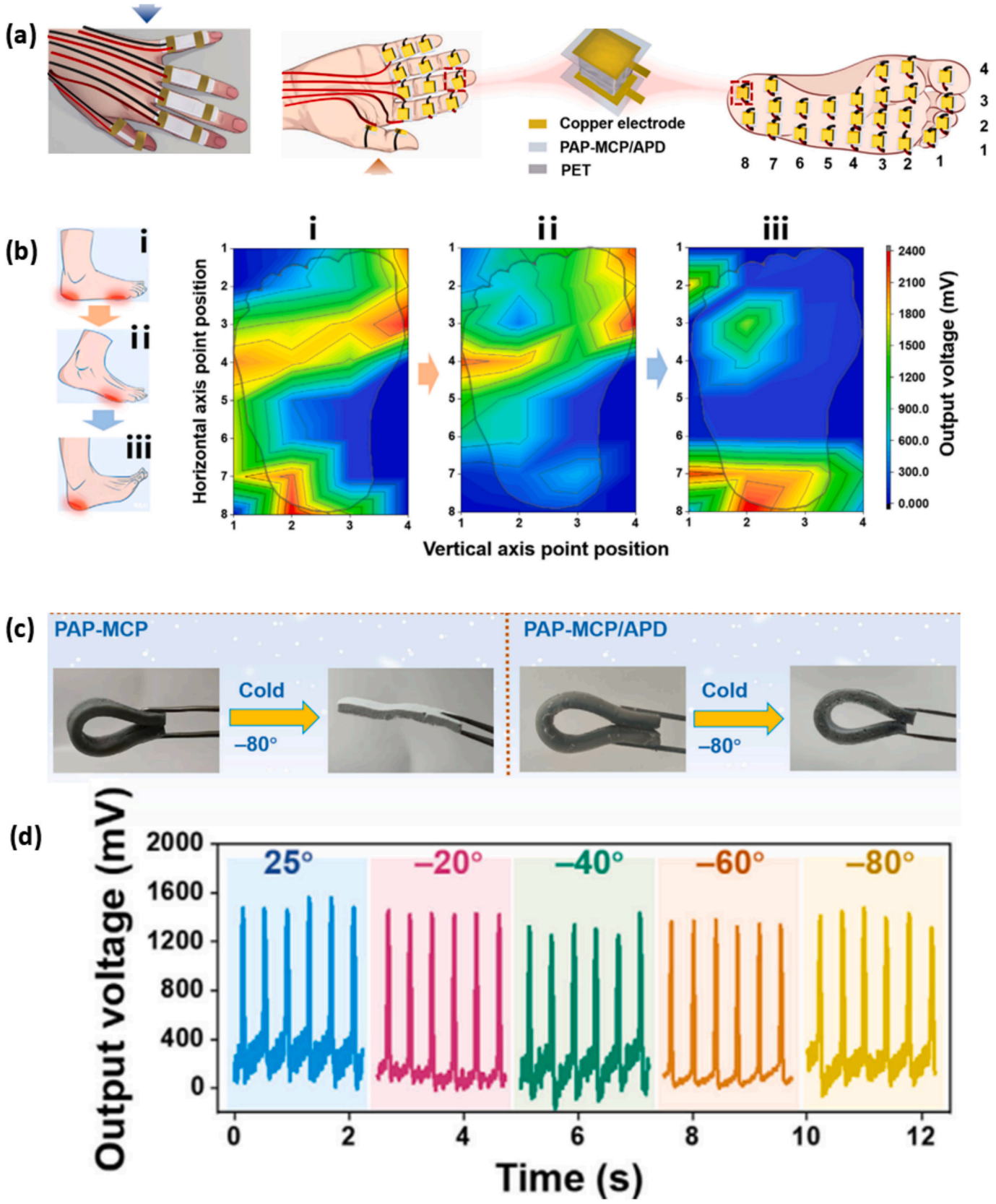


Fig. 13. Low-temperature rehabilitation monitoring using the PAP-MCP/APD hydrogel sensor. (a) Schematic of the rehabilitation-training system. (b) Voltage maps recorded for upright, forward-leaning, and backward-leaning postures. (c) Photographs of PAP-MCP and PAP-MCP/APD hydrogels after treatment at −80 °C, and (d) voltage responses of the PAP-MCP/APD sensor at temperatures from 25 to −80 °C. Reproduced with permission [108]. Copyright 2025, Wiley-VCH.

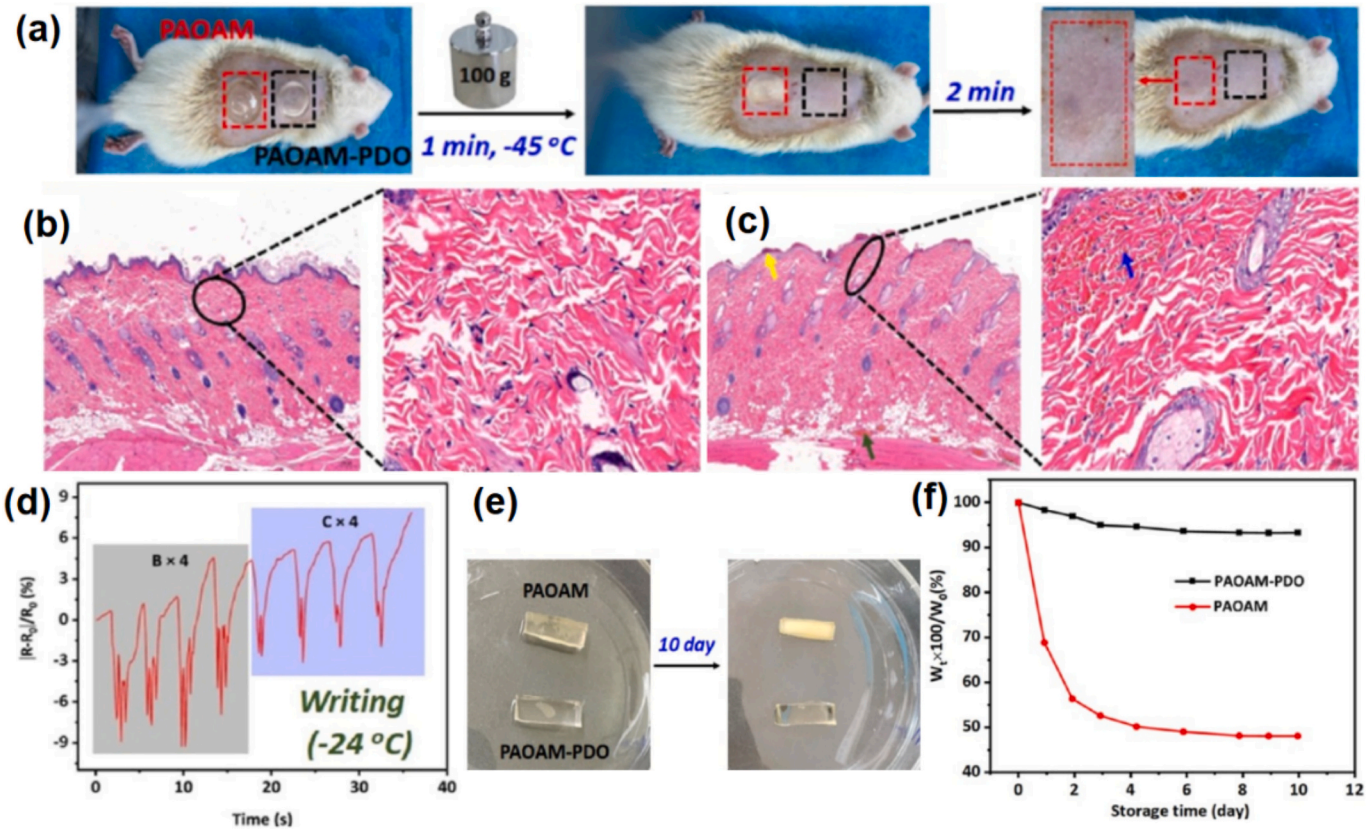


Fig. 14. Low-temperature protection, water retention, and motion sensing of PAOAM-PDO hydrogel devices. (a) Schematic of skin-mounted PAOAM and PAOAM-PDO devices at −24 °C; (b,c) hematoxylin and eosin (H&E)-stained skin sections after contact with the two hydrogels. (d) handwriting signals recorded at −24 °C, and (e,f) photographs and mass-retention results after 10 days at 25 °C and 60% RH. Reproduced with permission [109]. Copyright 2023, American Chemical Society.

autonomous closed-loop robotic control [115].

4.3. Translation progress and application bottlenecks

Recent analyses of lignocellulose-liquid-metal composites further indicate that renewable feedstocks can improve filler stabilization and multifunctional integration, promoting the industrialization of conductive hydrogel sensors, although feedstock variability, interfacial durability, scalable processing, and end-of-life recycling still act as restrictive factors [116]. Conductive hydrogel sensors have progressed from material characterization toward laboratory-scale device demonstrations. The PAHCT hydrogel sensor, with a swelling ratio of 5.5% after 48 h in seawater and stable output over 800 cycles, demonstrated joint-motion monitoring underwater and under simulated marine conditions [91]. The PAPL hydrogel electrode developed by Lv et al. showed no obvious signal drift after 2000 stretching cycles and produced ECG/EEG signals with signal-to-noise ratios superior to commercial Ag/AgCl electrodes, indicating potential for subsequent preclinical validation [111].

However, large-scale applications still face three major bottlenecks. First, advanced conductive fillers such as MXene and carbon nanotubes are difficult to manufacture. Their synthesis, purification, dispersion, and batch consistency add to the complexity. These factors also drive up costs. As a result, scalable processing and end-of-life management warrant further study [116]. Second, long-term service stability remains a major challenge. Conductive pathways are susceptible to gradual alteration. The main culprits include ion exchange, water loss or swelling, and interface aging. These degradation mechanisms are accelerated in seawater and other harsh media [91]. Third, integration with conventional electronics remains challenging, as electrode adhesion, encapsulation, and impedance mismatch can cause signal attenuation [95].

To address the integration issue, the THIN hydrogel-elastomer conductive nanomembrane developed by Jung et al. [110] reduced the interfacial impedance to 138.4 Ω at 1 kHz through a hydrogel–elastomer composite structure and enabled long-term monitoring (≥30 days) of dynamic electrical signals in rat myocardium, providing a device-integration strategy for soft bioelectronics. Biological compatibility also remains essential. Liu et al. [117] prepared a PVA-based hydrogel loaded with schisandrin B, showing a hemolysis ratio below 1%, cell viability above 99%, reduced interleukin-6 (IL-6) and tumor necrosis factor-α (TNF-α) expression, and a wound-healing rate of 93.56% at 7 days. Zhao et al. reported an oxidized-sodium-alginate/aminated-gelatin organohydrogel with no ice-crystal formation from −60 °C to 20 °C and cell viability above 80% [109]. These results support material-level compatibility, while integrated devices still require packaging, sterilization, chronic tissue-response, and calibration-stability evaluation.

5. Conclusions and future perspectives

The core of sensing applications lies in synergistic optimization. This involves water molecule management, network topology regulation, and multiple dynamic crosslinking. Such microstructural design ensures both structural integrity and stable ionic/electronic transport. These benefits hold under complex conditions, including temperature fluctuations, humidity variations, solution erosion, mechanical deformation, and even biological fluids. Thus, This review systematically summarizes two key aspects. The first is transduction mechanisms of conductive hydrogels, including resistance-based, piezoionic, thermoresistive, and ionic thermoelectric types. The second is mainstream strategies for

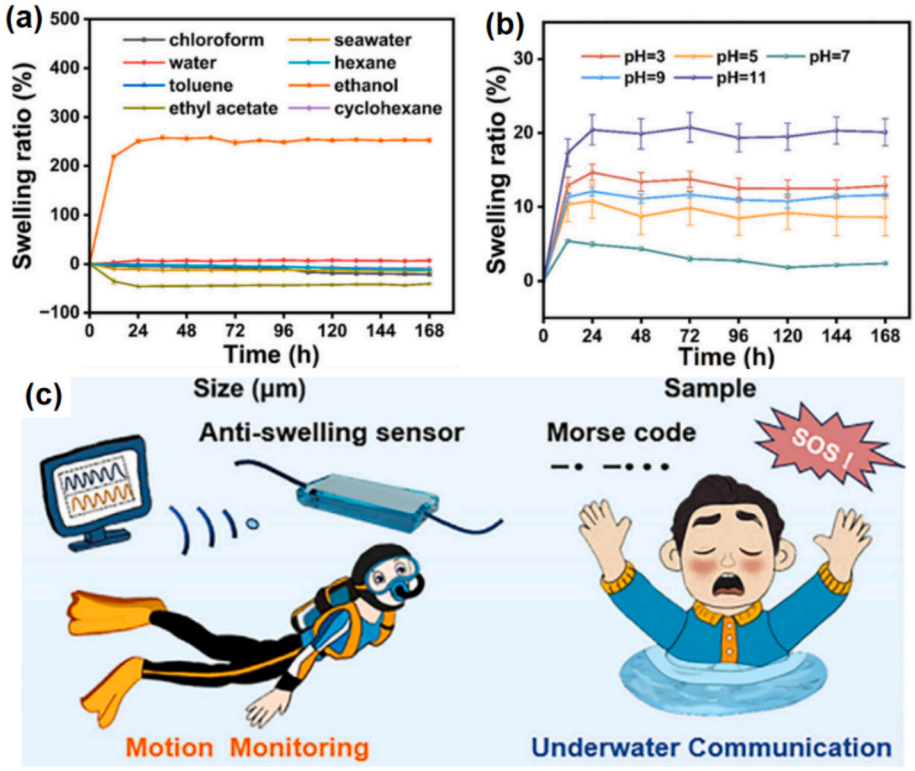


Fig. 15. Chemical stability, volume stability, and underwater sensing demonstrations of PAHCT hydrogel transducers: (a) swelling in seawater and selected chemical media, (b) swelling ratios under different solution conditions, (c) underwater joint-motion sensing and Morse-code communication. Reproduced with permission [91]. Copyright 2025, Wiley-VCH.

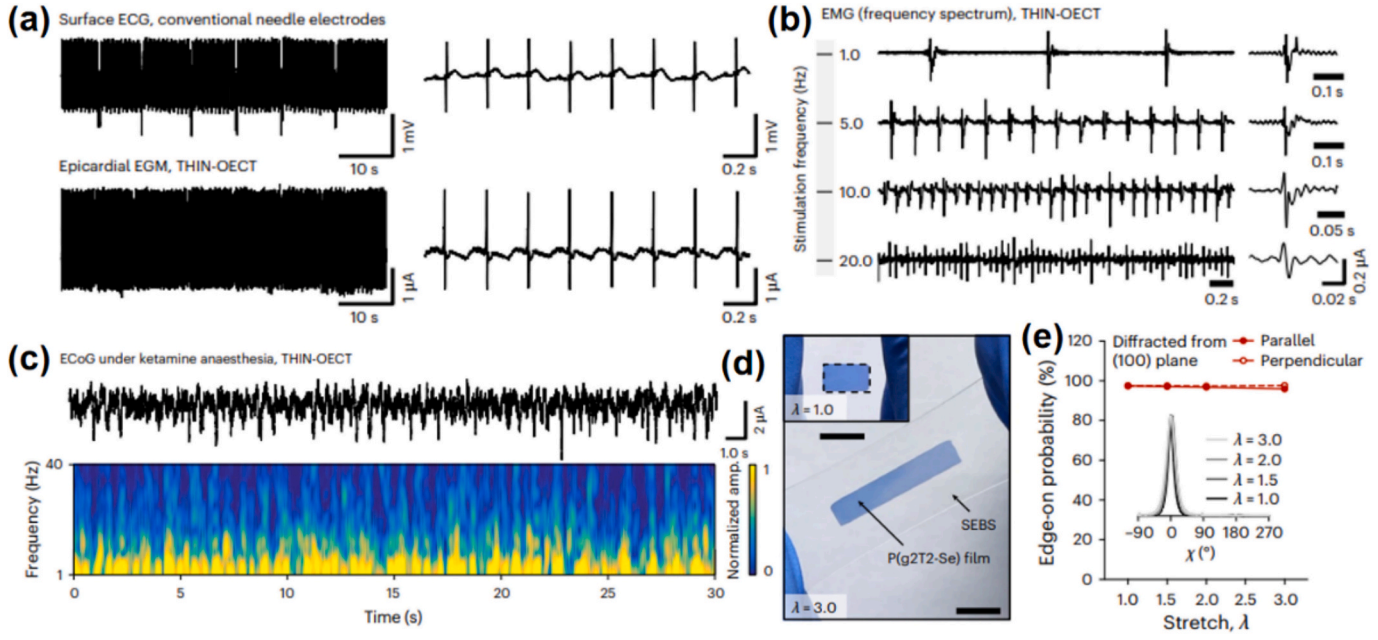


Fig. 16. Electrophysiological recording using THIN hydrogel–elastomer conductive nanomembranes: (a) electrocardiogram (ECG) and epicardial recordings, (b) electrically stimulated EMG, (c) cortical-potential waveforms and time–frequency maps, (d) P(g_2T_2-Se)/styrene–ethylene–butylene–styrene (SEBS) layers at 0% and 200% strain, (e) strain-dependent crystalline alignment. Reproduced with permission [110]. Copyright 2025, Springer Nature.

enhancing environmental adaptability. These strategies target anti-freezing, anti-drying, anti-swelling, anti-corrosion, and stretchability. For anti-freezing and water retention, high-concentration salts or organic solvents are used to disrupt the hydrogen bonding network of water molecules. For anti-swelling and anti-corrosion, dense double networks, hydrophobic coatings, or metal-coordination crosslinking are constructed to inhibit swelling and ion erosion. For stretchability and fatigue resistance, dynamic hydrogen bonds, hydrophobic aggregates, or sliding ring structures are introduced to achieve low hysteresis and high fatigue resistance under large strains. The above strategies are unified by

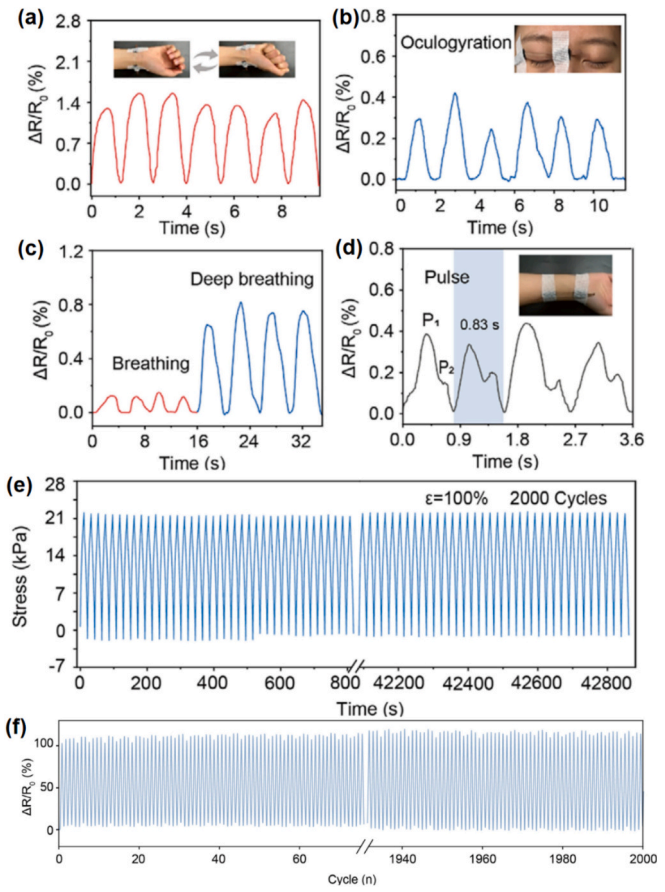


Fig. 17. Functional sensing and cycling durability of the PAPL conductive hydrogel: (a) fist contraction, (b) ocular micromovement, (c) respiration, (d) arterial pulsation, (e) 2000 tensile cycles at 100% strain, (f) normalized resistance after cycling. Reproduced with permission [111]. Copyright 2025, Wiley-VCH.

a core principle of "component complementarity and network adaptation." By rationally combining ion hydration, hydrogen bonding networks, metal coordination, and interfacial encapsulation, the hydrogel achieves stable and sensitive sensing outputs under a wide range of extreme conditions, including from −80 °C to elevated temperatures, from dry to humid environments, from freshwater to seawater, and under both static and dynamic large deformations. Based on these performance breakthroughs, conductive hydrogels have expanded from human motion monitoring to diverse application scenarios such as underwater Morse code communication, visual feedback for rehabilitation training, self-powered triboelectric nanogeneration, epicardial electrophysiological recording, and electrocorticogram monitoring. Although current research has significantly improved the extreme environmental adaptability of conductive hydrogels, their scalability and commercialization for practical applications still face ongoing challenges. Future efforts should focus on breakthroughs in the following five directions to advance them toward a new stage featuring higher integration, a wider operating range, and a longer service life (Fig. 18).

From an engineering perspective, the critical challenge is to retain calibrated sensing performance after material integration and prolonged service, rather than to maximize a single peak property. Scale-up requires batch-reproducible precursor formulation, controllable network thickness, continuous or roll-compatible processing, and quantified manufacturing yield. Device packaging must suppress dehydration, swelling, and chemical ingress while preserving breathability, conformability, and analyte transport. Electrode and interconnect adhesion, contact impedance, hysteresis, signal drift, and coupled temperature–humidity–chemical aging should be evaluated at the device level. Common definitions of failure, standardized conditioning and cycling protocols, accelerated-aging models linked to service-life prediction, sterilization and biological qualification, and transparent cost and life cycle assessments are also needed before reliable commercialization.

(1) Establishing environment-property-structure correlation models

From the perspective of material design, current protection strategies under coupled multiple extreme environments urgently need to shift from passive resistance to active adaptation as a theoretical paradigm. To address the failure behaviors of hydrogels under multi-factor coupled

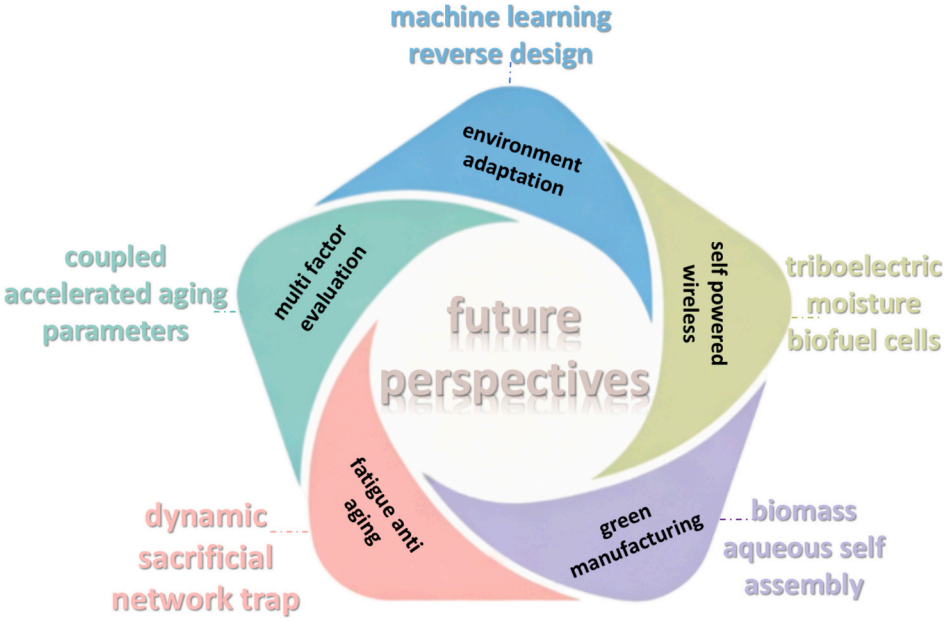


Fig. 18. Future perspectives for conductive hydrogel sensing applications: environment-property-structure correlation models, energy harvesting and wireless transmission, green low-energy manufacturing, fatigue resistance/anti-aging, and multi-factor accelerated aging evaluation.

environments such as low temperature, high humidity, corrosion, and stretching, a reverse design platform driven by the synergy of molecular dynamics simulations and machine learning can be constructed. By simulating and analyzing failure mechanisms including chain segment freezing, swelling-induced stress concentration, and corrosive ion diffusion, a correlation library between failure modes and structural descriptors can be established. On this basis, a new dual-mode design concept combining topological mismatch buffering and sacrificial domain rearrangement can be further proposed. The former introduces heterogeneous crosslinking or block topological mismatch into the polymer network to form local strain-dissipating microdomains, thereby inhibiting the propagation of fatigue cracks. The latter mimics the damage rearrangement mechanism of biological tissues, triggering selective rupture and dynamic rearrangement of reversible sacrificial bonds such as hydrogen bonds and metal coordination bonds under extreme environments, converting the volume expansion energy induced by frost heave or corrosion into a driving force for network reconfiguration. Combined with Bayesian optimization for high-throughput screening of composition and topology, multi-objective synergistic optimization of anti-freezing, anti-swelling, and anti-fatigue properties can be achieved. The resulting environment-adaptive dynamic network design model can not only overcome the bottleneck of difficult synergy among multiple properties in conventional hydrogels but also be extended to the systematic protective design of other soft matter materials under complex service environments.

(2) Integrating energy harvesting and wireless transmission

From an application design perspective, to address the two core bottlenecks commonly encountered in wearable and implantable medical devices under coupled multiple extreme environments, namely impedance mismatch and power supply dependency, a new concept of a hydrogel system integrating environment-adaptive energy and closed-loop sensing is proposed. A multifunctional hydrogel serves as the core component. It provides anti-freezing, anti-swelling, and anti-fatigue properties. This hydrogel acts as both the sensing medium and the energy conversion unit. By integrating triboelectric, moisture-enabled, and biofuel cell energy harvesters, a multimodal complementary micro-energy module is constructed. This enables the system to autonomously switch its power supply mode according to environmental conditions under low-temperature, high-humidity, or corrosive environments, thereby reducing dependence on external power sources. To address the impedance mismatch issue, a conformal hydrogel electrode with gradient conductivity and a stretchable skin-friendly interface can be designed. By regulating the percolation network and interfacial wettability, dynamic impedance matching with human tissues and electronic circuits can be achieved, thereby minimizing motion artifacts and interfacial noise. The resulting "self-powered, self-adaptive, self-transmitting" smart medical patch system is expected to provide a maintenance-free and environmentally robust new application solution for long-term bedridden care, polar operations, or battlefield casualty monitoring.

(3) Developing green macromolecules and low-energy-consumption manufacturing

Green macromolecules and low-energy manufacturing are driving forces behind this work. However, current hydrogels rely on toxic crosslinkers, energy-intensive processing, and non-degradable monomers. These problems are magnified under coupled multiple extreme environments. We therefore propose an integrated design concept based on biomass source, aqueous self-assembly, and closed-loop regeneration. Natural macromolecules such as cellulose, silk fibroin, and sodium alginate serve as the primary building blocks. Bioinspired small molecules like gallic acid and lipoic acid are also incorporated. Through the synergistic driving of dynamic covalent bonds and multiple hydrogen bonds, rapid self-assembly is achieved in aqueous phase at room temperature and atmospheric pressure. This approach completely eliminates the need for organic solvents and high-temperature thermal curing. Furthermore, biomimetic anti-freezing and anti-swelling modules are introduced to encode environmental adaptability directly into the macromolecular sequence, avoiding additional chemical waste from post-synthesis functional modifications. Meanwhile, a triggerable degradation–recycling loop is constructed, in which the dynamic network dissociates through pH or ionic strength regulation after service, and the recovered monomers or oligomers are used for secondary reassembly, forming a material cycle with low entropy loss. In addition, the low-energy manufacturing plays a key role. Aqueous extrusion-based 3D printing and microfluidic spinning are two examples. They help green the entire life cycle of hydrogels from raw materials to synthesis to processing. This approach embodies a sustainable philosophy: "from nature, back to nature," which is especially relevant for hydrogels used in extreme environments.

(4) Enhancing fatigue resistance and anti-aging capability for long-term service

A durability design concept is proposed for hydrogels in extreme environments. It focuses on fatigue resistance and anti-aging for long-term use. The concept addresses network degradation, chain fracture, and performance decline. It integrates three strategies: sacrificial bonds, radical traps, and entropic elasticity. Sacrificial bonds are introduced as energy dissipation units. These include hydrogen bonds, metal coordination, or dynamic covalent bonds. They break under cyclic loading to absorb strain energy. They then reform upon unloading to repair microdamage, preventing crack growth. To combat aging, radical scavengers and UV absorbers are grafted onto the network. These endogenous traps capture reactive oxygen species, blocking chain degradation. This protects against oxidation, hydrolysis, and UV damage. Entropic recovery structures are also incorporated. Liquid crystal elastomers or slide-ring topologies are typical examples. They restore network configuration after large deformation, minimizing chain slip and residual stress. Accelerated aging tests and machine learning models are used together. This allows synergistic optimization under multiple factors. The result is reduced degradation of mechanical and functional performance over time. This framework offers a systematic guideline for designing durable soft materials for extreme environments.

(5) Establishing a multi-factor accelerated aging evaluation system

From the perspective of standardized evaluation, to address the lack of a unified certification basis for the long-term reliability of conductive hydrogels under coupled multiple extreme environmental factors, a framework for constructing a multi-factor coupled accelerated aging evaluation system is proposed. On this basis, physics-of-failure and machine learning methods are integrated. The resulting model quantifies how environmental loads drive performance degradation. It allows extrapolation from accelerated experiments to real-world long-term service. A multi-factor aging evaluation standard is then formulated. This standard is objective, reproducible, and comparable. It unifies reliability certification for conductive hydrogels across diverse applications, effectively bridging the gap between laboratory research and industrial deployment.

In summary, conductive hydrogels have demonstrated substantial potential for transitioning from functional materials toward intelligent systems in the field of extreme-environment sensing. With sustained breakthroughs in intelligent design, self-powered integration, green manufacturing, dynamic self-healing, and standardized evaluation, their practical applications in strategic domains such as marine exploration, polar scientific research, deep-space exploration, implantable medicine, and human–machine interaction will soon become a reality.

CRediT authorship contribution statement

Yuying Wu: Writing – review & editing, Writing – original draft, Methodology, Funding acquisition, Visualization. **Cifang Jiang:** Writing – original draft, Writing – review & editing. **Gang Zhou:** Formal analysis, Funding acquisition. **Xinyuan Zhu:** Writing – review & editing. **Youfu Wang:** Writing – review & editing.

Declaration of competing interest

The authors declare that they have no known competing financial interests or personal relationships that could have appeared to influence the work reported in this paper.

Acknowledgements

This review was supported by National Natural Science Foundation of China (12204301, 52102237).

Data availability

No data was used for the research described in the article.

References

[1] C. Sun, C. Hou, H. Zhang, Y. Li, Q. Zhang, H. Wang, Ultra-stretchable, self-adhesive, transparent, and ionic conductive organohydrogel for flexible sensor, APL Mater. 9 (2021) 011101.
[2] Y. Liu, M. Pharr, G.A. Salvatore, Lab-on-skin: a review of flexible and stretchable electronics for wearable health monitoring, ACS Nano 11 (2017) 9614–9635.
[3] M. Yuan, Y. Long, T. Liu, J. Liu, S. Qiu, T. Lin, F. Xu, Y. Fang, Soft electronics for advanced infant monitoring, Mater. Today 75 (2024) 166–186.
[4] V. Vallem, Y. Sargolzaeiaval, M. Ozturk, Y.C. Lai, M.D. Dickey, Energy harvesting and storage with soft and stretchable materials, Adv. Mater. 33 (2021) 2004832.
[5] Y. Zou, P. Tan, B. Shi, H. Ouyang, D. Jiang, Z. Liu, H. Li, M. Yu, C. Wang, X. Qu, A bionic stretchable nanogenerator for underwater sensing and energy harvesting, Nat. Commun. 10 (2019) 2695.
[6] Y.H. Jung, S.K. Hong, H.S. Wang, J.H. Han, T.X. Pham, H. Park, J. Kim, S. Kang, C.D. Yoo, K.J. Lee, Flexible piezoelectric acoustic sensors and machine learning for speech processing, Adv. Mater. 32 (2020) 1904020.
[7] Q. Xu, J. Wen, Y. Qin, Development and outlook of high output piezoelectric nanogenerators, Nano Energy 86 (2021) 106080.
[8] S. Geng, S. Fan, H. Li, Y. Qi, C. An, E. Wu, J. Su, J. Liu, An artificial neuromuscular system for bimodal human–machine interaction, Adv. Funct. Mater. 33 (2023) 2302345.
[9] Y. Gu, Y. Luo, Q. Guo, W. Yu, P. Li, X. Wang, T. Ye, H. Chang, W. Yuan, H. Wu, Empowering human-machine interfaces: self-powered hydrogel sensors for flexible and intelligent systems, Adv. Funct. Mater. 36 (2026) e09085.
[10] C. Zhang, Z. Jiang, M. Sun, R. Augustin-Lawson, S.H. Kwon, L. Dong, Nature-inspired helical piezoelectric hydrogels for energy harvesting and self-powered human-machine interfaces, Nano Energy 136 (2025) 110755.
[11] Y. Zhang, Z. Xu, Y. Yuan, C. Liu, M. Zhang, L. Zhang, P. Wan, Flexible antiswelling photothermal-therapy MXene hydrogel-based epidermal sensor for intelligent human–machine interfacing, Adv. Funct. Mater. 33 (2023) 2300299.
[12] X. Dai, Y. Wu, Q. Liang, J. Yang, L.B. Huang, J. Kong, J. Hao, Soft robotic-adapted multimodal sensors derived from entirely intrinsic self-healing and stretchable cross-linked networks, Adv. Funct. Mater. 33 (2023) 2304415.
[13] W. Liu, Y. Duo, X. Chen, B. Chen, T. Bu, L. Li, J. Duan, Z. Zuo, Y. Wang, B. Fang, An intelligent robotic system capable of sensing and describing objects based on bimodal, self-powered flexible sensors, Adv. Funct. Mater. 33 (2023) 2306368.
[14] L. Chen, Z. Jin, W. Feng, L. Sun, H. Xu, C. Wang, A hyperelastic hydrogel with an ultralarge reversible biaxial strain, Science 383 (2024) 1455–1461.
[15] Z. Fu, H. Liu, Q. Lyu, J. Dai, C. Ji, Y. Tian, Anti-freeze hydrogel-based sensors for intelligent wearable human-machine interaction, Chem. Eng. J. 481 (2024) 148526.
[16] Z. Huang, Y. Zhu, F. Qiu, X. Que, H. Sun, Z. Zhang, Y. Wu, Multiscale cellulose-based functional materials for advanced flexible electronics, Macromol. Rapid Commun. 46 (2025) 202500710.
[17] R. Venkatesan, T. Dhilipkumar, A.G. Al-Sehemi, Y.A. Kumar, S.-C. Kim, Recent advances in structural color materials based on flexible cellulose nanocrystals, Cellulose 31 (2024) 4681–4708.
[18] C. Zhu, J. Wu, J. Yan, X. Liu, Advanced fiber materials for wearable electronics, Adv. Fiber Mater. 5 (2022) 12–35.
[19] S. Bauer, S. Bauer-Gogonea, I. Graz, M. Kaltenbrunner, C. Keplinger, R. Schwödiauer, 25th anniversary article: a soft future: from robots and sensor skin to energy harvesters, Adv. Mater. 26 (2014) 149–162.
[20] K. Jang, K. Li, H. Chung, S. Xu, H. Jung, Y. Yang, J. Kwak, H. Jung, J. Song, C. Yang, Self-assembled three dimensional network designs for soft electronics, Nat. Commun. 8 (2017) 15894.
[21] Y. Zhang, Y. Liu, Y. Lu, S. Gong, H. Haick, W. Cheng, Y. Wang, Tailor-made gold nanomaterials for applications in soft bioelectronics and optoelectronics, Adv. Mater. 36 (2024) 2405046.
[22] J. Heikenfeld, A. Jajack, J. Rogers, P. Gutruf, L. Tian, T. Pan, R. Li, M. Khine, J. Kim, J. Wang, Wearable sensors: modalities, challenges, and prospects, Lab Chip 18 (2018) 217–248.
[23] E.M. Ahmed, Hydrogel: preparation, characterization, and applications: a review, J. Adv. Res. 6 (2015) 105–121.
[24] P. Patel, P. Thareja, Hydrogels differentiated by length scales: a review of biopolymer-based hydrogel preparation methods, characterization techniques, and targeted applications, Eur. Polym. J. 163 (2022) 110935.
[25] T. Zhang, R. Zhang, C. Zhao, Z. Li, L. Wang, H. Zhao, Preparation, characterization, multidimensional applications and prospects of protein bio-based hydrogels: a review, Int. J. Biol. Macromol. 312 (2025) 144199.
[26] S. Khan, A. Ullah, K. Ullah, N.-u. Rehman, Insight into hydrogels, Des. Monomers Polym. 19 (2016) 456–478.
[27] E.S. Lee, M.Y. Lee, D.H. Kim, J.H. Koo, Recent advances in hydrogel-based soft bioelectronics and its convergence with machine learning, Adv. Eng. Mater. 26 (2024) 2401432.
[28] Y. Ai, Z. Lin, W. Zhao, M. Cui, W. Qi, R. Huang, R. Su, Nanocellulose-based hydrogels for drug delivery, J. Mater. Chem. B 11 (2023) 7004–7023.
[29] L. Dinh, S.-J. Hwang, B. Yan, Hydrogel conjugation: engineering of hydrogels for drug delivery, Pharmaceutics 17 (2025) 897.
[30] J. Li, D.J. Mooney, Designing hydrogels for controlled drug delivery, Nat. Rev. Mater. 1 (2016) 16071.
[31] T. Yeruva, S. Yang, S. Doski, G.A. Duncan, Hydrogels for Mucosal Drug Delivery, ACS Appl. Bio Mater. 6 (2023) 1684–1700.
[32] G. Sun, Z. Sun, L. Liu, P. Wang, Z. Zhang, Z. Li, C. Meng, S. Guo, Transparent conductive hydrogels with water-responsive contractility, repairability, and biocompatibility for visible conformal shape-adaptive tissue-adherent monitoring, Adv. Funct. Mater. 36 (2026) e22718.
[33] Y. Mo, M. Zhu, S. Sun, D. Sun, D. Lu, Microgel double-crosslinked hydrogel with excellent mechanical properties for flexible electronics, J. Colloid Interface Sci. 699 (2025) 138155.
[34] Y. Huang, Y. Yang, Y. Yang, S. Chen, S. Liu, X. Zhang, Self-healing, high mechanical strength and adhesive supramolecular hydrogel based on triblock copolymer for flexible electronics, Polymer 318 (2025) 127966.
[35] W. Che, X. He, X. Zheng, K. Wang, J. Shi, Z. Song, B. Liu, X. Zeng, M. Zuo, Rational design of anti-freezing dual-network hydrogels with superior mechanical and self-healing properties for advanced flexible electronics, Chem. Eng. J. 515 (2025) 163607.
[36] Y. Jian, S. Handschuh-Wang, J. Zhang, W. Lu, X. Zhou, T. Chen, Biomimetic anti-freezing polymeric hydrogels: keeping soft-wet materials active in cold environments, Mater. Horiz. 8 (2021) 351–369.
[37] S. Huang, S.U. Villafranca, I. Mehta, O. Yosfan, E. Hong, A. Wang, N. Wu, Q. Wang, S. Rao, A nanoscale inorganic coating strategy for stabilizing hydrogel neural probes in vivo, J. Mater. Chem. B 11 (2023) 7629–7640.
[38] Y. Yu, G. Huang, H. Miao, J. Liang, X. Zhang, Y. Liu, L. Tong, C. Dong, X. Fu, H. Huang, Confined water molecules of ionic conductive hydrogel electrolyte for the high-performance, dendrite-free, and safe flexible supercapacitor, ACS Appl. Energy Mater. 8 (2025) 11706–11708.
[39] X. Di, J. Li, M. Yang, Q. Zhao, G. Wu, P. Sun, Bioinspired, nucleobase-driven, highly resilient, and fast-responsive antifreeze ionic conductive hydrogels for durable pressure and strain sensors, J. Mater. Chem. A 9 (2021) 20703–20713.
[40] S.-N. Li, X.-F. He, Z.-F. Zeng, B. Jiang, Q. Wu, L.-X. Gong, Y. Li, J. Bae, S. Wang, L.-C. Tang, Mechanically ductile, ionically conductive and low-temperature tolerant hydrogel enabled by high-concentration saline towards flexible strain sensor, Nano Energy 103 (2022) 107789.
[41] X.P. Morelle, W.R. Illeperuma, K. Tian, R. Bai, Z. Suo, J.J. Vlassak, Highly stretchable and tough hydrogels below water freezing temperature, Adv. Mater. 30 (2018) 1801541.
[42] H. Jiang, C. Ou, D. Zhang, X. Hu, Y. Ma, M. Wang, Y. Huang, L. Xiao, Tough ion-conductive hydrogel with anti-dehydration as a stretchable strain sensor for gesture recognition, ACS Appl. Polym. Mater. 5 (2023) 6828–6841.
[43] B. Xu, Y. Liu, L. Wang, X. Ge, M. Fu, P. Wang, Q. Wang, High-strength nanocomposite hydrogels with swelling-resistant and anti-dehydration properties, Polymers 10 (2018) 1025.
[44] Z. Sun, C. Dong, B. Chen, W. Li, H. Hu, J. Zhou, C. Li, Z. Huang, Strong, tough, and anti-swelling supramolecular conductive hydrogels for amphibious motion sensors, Small 19 (2023) 2303612.
[45] Q. Yang, B. Lin, J. Tang, Y. Wang, H. Zheng, H. Zhang, Z. Nie, Y. Zhang, A pH-controlled solid inhibitor based on PAM hydrogel for steel corrosion protection in wide range pH NaCl medium, Molecules 28 (2023) 1314.
[46] H. Zhang, M. Yue, T. Wang, J. Wang, X. Wu, S. Yang, Conductive hydrogel-based flexible strain sensors with superior chemical stability and stretchability for mechanical sensing in corrosive solvents, New J. Chem. 45 (2021) 4647–4657.
[47] D. Chimene, R. Kaunas, A.K. Gaharwar, Hydrogel bioink reinforcement for additive manufacturing: a focused review of emerging strategies, Adv. Mater. 32 (2020) 1902026.
[48] S. Duan, M. Hua, C.W. Zhang, W. Hong, Y. Yan, A. Jazzar, C. Chen, P. Shi, M. Si, D. Wu, Z. Lin, P. He, Y. Du, X. He, Noncovalent aggregation for diverse properties in hydrogels: a comprehensive review, Chem. Rev. 125 (2025) 7918–7964.

[49] Q. Chen, M. Chen, D.-H. Qu, Dynamic self-healing polymer architectures for high-performance flexible sensing, Adv. Mater. 38 (2026) 73777.
[50] R. Xu, H.S. Ooi, L. Bian, L. Ouyang, W. Sun, Dynamic hydrogels for biofabrication: a review, Biomaterials 320 (2025) 123266.
[51] L. Jiang, Z. Sha, Y. Zheng, R. Zhu, C. Yu, Q. Chen, R. Ran, W. Cui, Bioinspired hydrogels thriving in harsh conditions: where soft materials conquer hard challenges, Prog. Mater. Sci. 152 (2025) 101459.
[52] Y. Chang, Y. Jia, Y. Pan, J. Wang, H. Yang, M. Zu, H. Cheng, Enhancing water retention in hydrogels under extreme conditions: strategies, applications and challenges, Mater. Sci. Eng. R. Rep. 167 (2026) 101098.
[53] Y. Gu, Y. Luo, Q. Guo, W. Yu, P. Li, X. Wang, T. Ye, H. Chang, W. Yuan, H. Wu, J. Wu, K. Tao, Empowering human-machine interfaces: self-powered hydrogel sensors for flexible and intelligent systems, Adv. Funct. Mater. 36 (2026) e09085.
[54] B. Chen, Z. Feng, F.-Z. Yao, M.-H. Zhang, K. Wang, Y. Wei, W. Gong, J. Rödel, Flexible piezoelectrics: integration of sensing, actuating and energy harvesting, NPJ Flexible Electron. 9 (2025) 58.
[55] M. Zhao, Z. Tang, X. Zhang, Z. Li, H. Xiao, M. Zhang, K. Liu, Y. Ni, L. Huang, L. Chen, A self-healing, stretchable, and conductive poly(N-vinylpyrrolidone)/gallic acid composite hydrogel formed via hydrogen bonding for wearable electronic sensors, Compos. Sci. Technol. 198 (2020) 108294.
[56] Y. Yang, Y. Yang, Y. Cao, X. Wang, Y. Chen, H. Liu, Y. Gao, J. Wang, C. Liu, W. Wang, Anti-freezing, resilient and tough hydrogels for sensitive and large-range strain and pressure sensors, Chem. Eng. J. 403 (2021) 126431.
[57] B. Du, Y. Chao, K. Yang, B. Li, R. Luo, S. Zhou, H. Li, Stretchable and tough tannic acid-modified graphene oxide/ polyvinyl alcohol conductive hydrogels for strain and pressure sensors, AIP Adv. 12 (2022) 095206.
[58] R. Cheng, X. Zhang, J. Li, H. Zheng, Q. Zhang, Nanoporous, Ultrastiff, and transparent plastic-like polymer hydrogels enabled by hydrogen bonding-induced self-assembly, ACS Appl. Mater. Interfaces 16 (2024) 42783–42793.
[59] H. Huo, J. Shen, J. Wan, H. Shi, H. Yang, X. Duan, Y. Gao, Y. Chen, F. Kuang, H. Li, A tough and robust hydrogel constructed through carbon dots induced crystallization domains integrated orientation regulation, Nat. Commun. 16 (2025) 6221.
[60] X. Liu, Z. Guo, J. Wang, W. Shen, Z. Jia, S. Jia, L. Li, J. Wang, L. Wang, J. Li, Thiolation-based protein–protein hydrogels for improved wound healing, Adv. Healthc. Mater. 13 (2024) 2303824.
[61] G. Prakash, A.J. Clasky, K. Gadani, M. Nazeri, F.X. Gu, Ion-mediated cross-linking of hyaluronic acid into hydrogels without chemical modification, Biomacromolecules 25 (2024) 7723–7735.
[62] S. Bunuasunthon, M. Nakamoto, V.P. Hoven, M. Matsusaki, Construction of tough hydrogel cross-linked via ionic interaction by protection effect of hydrophobic domains, ACS Biomater. Sci. Eng. 10 (2024) 4245–4258.
[63] P.I. Sepulveda-Medina, C. Wang, R. Li, M. Fukuto, B.D. Vogt, Influence of the nature of aliphatic hydrophobic physical crosslinks on water crystallization in copolymer hydrogels, J. Phys. Chem. B 126 (2022) 5544–5554.
[64] L. Voorhaar, R. Hoogenboom, Supramolecular polymer networks: hydrogels and bulk materials, Chem. Soc. Rev. 45 (2016) 4013–4031.
[65] A. Sawut, R. Simayi, X. Zhang, M. Jiang, Z. Zhu, T. Wu, Preparation, properties, self crosslinking mechanism, and characterization of UV initiated polyacrylic acid superabsorbent resins, Polym. Adv. Technol. 33 (2022) 3666–3680.
[66] C. Erkoc, E. Yildirim, M. Yurtsever, O. Okay, Roadmap to design mechanically robust copolymer hydrogels naturally cross-linked by hydrogen bonds, Macromolecules 55 (2022) 10576–10589.
[67] Y. Yan, X. Zhang, C. Xiao, X. Chen, Knoevenagel condensation reaction-empowered hydrogels with pH-tunable dynamic properties, ACS Macro Lett. 14 (2025) 773–780.
[68] C. Bahou, R.J. Spears, A.M. Ramírez Rosales, L.N.C. Rochet, L.J. Barber, K. S. Stankevich, J.F. Miranda, T.C. Butcher, A.M. Kerrigan, V.K. Lazarov, Hydrogel cross-linking via thiol-reactive pyridazinediones, Biomacromolecules 24 (2023) 4646–4652.
[69] Q. Chen, B. Chen, S. Xiao, J. Feng, J. Yang, Q. Yue, X. Zhang, T. Wang, Giant Thermopower of hydrogen ion enhanced by a strong hydrogen bond system, ACS Appl. Mater. Interfaces 14 (2022) 19304–19314.
[70] D. Fu, Y. Lu, Z. Peng, W. Zhong, A zwitterionic hydrogel with a surprising function of increasing the ionic conductivity of alkali metal chloride or sulfuric acid water-soluble electrolyte, J. Mater. Chem. A 11 (2023) 13543–13551.
[71] J. Zhao, Y. Lu, Y. Liu, L. Liu, J. Yin, B. Sun, G. Wang, Y. Zhang, A self-healing PVA-linked phytic acid hydrogel-based electrolyte for high-performance flexible supercapacitors, Nanomaterials (Basel, Switzerland) 13 (2023) 380.
[72] S. Wang, L. Yu, S. Wang, L. Zhang, L. Chen, X. Xu, Z. Song, H. Liu, C. Chen, Strong, tough, ionic conductive, and freezing-tolerant all-natural hydrogel enabled by cellulose-bentonite coordination interactions, Nat. Commun. 13 (2022) 3408.
[73] X. Wang, X. Wang, M. Pi, R. Ran, High performance double conductive network hydrogel based on soaking strategy for supercapacitors, Macromol. Mater. Eng. 307 (2021) 2100652.
[74] Z. Wu, L. Rong, J. Yang, Y. Wei, K. Tao, Y. Zhou, B.R. Yang, X. Xie, J. Wu, Ion-conductive hydrogel-based stretchable, self-healing, and transparent NO2 sensor with high sensitivity and selectivity at room temperature, Small 17 (2021) 2104997.
[75] J. Yang, L. Chang, C. Ma, Z. Cao, H. Liu, Highly electrically conductive flexible ionogels by drop-casting ionic liquid/PEDOT:PSS composite liquids onto hydrogel networks, Macromol. Rapid Commun. 43 (2022) 202100557.
[76] J. Xu, C.-H. Tai, T.-Y. Chen, S.-h. Hsu, An anti-inflammatory electroconductive hydrogel with self-healing property for the treatment of Parkinson's disease, Chem. Eng. J. 446 (2022) 137180.
[77] L. Jiang, S. He, A. Liu, J. Zhang, J. Liu, S. He, W. Shao, Preparation and characterization of self-healable and wearable hydrogels with ultrasensitive sensing performances, Compos. Part B Eng. 239 (2022) 109982.
[78] Y. Lu, S. Li, Y. Ma, F. Deng, Y. Yue, S. Jiang, M. Ye, Y. Zhou, H. Xiao, J. Han, Nanocellulose-assisted construction of conductive gradient hydrogel for remote actuated and self-sensing soft actuator, Carbohydr. Polym. 368 (2025) 124092.
[79] S. Li, H. Yang, N. Zhu, G. Chen, Y. Miao, J. Zheng, Y. Cong, Y. Chen, J. Gao, X. Jian, et al., Biotissue-inspired anisotropic carbon fiber composite hydrogels for logic gates, integrated soft actuators, and sensors with ultra-high sensitivity, Adv. Funct. Mater. 33 (2022) 2211189.
[80] X. Kang, X. Li, C. Liu, M. Cai, P. Guan, Y. Luo, Y. Guan, Y. Tian, K. Ren, C. Ning, et al., A shape-persistent Plasticine-like conductive hydrogel with self-healing properties for peripheral nerve regeneration, J. Mater. Sci. Technol. 142 (2023) 134–143.
[81] H. He, Y. Chen, A. Pu, L. Wang, W. Li, X. Zhou, C.Y. Tang, K. Ban, M. Yang, L. Xu, Strong and high-conductivity hydrogels with all-polymer nanofibrous networks for applications as high-capacitance flexible electrodes, NPJ Flexible Electron. 8 (2024) 56.
[82] J. Yin, P. Jia, Z. Ren, Q. Zhang, W. Lu, Q. Yao, M. Deng, X. Zhou, Y. Gao, N. Liu, Recent advances in self-powered sensors based on ionic hydrogels, Research 8 (2025) 0571.
[83] Y. Zhong, L. Ma, P. He, Q. Zhao, J. Li, Hybrid piezo/triboelectric Nanogenerators based on Nanofibrous aerogels for energy harvesting and respiratory monitoring, ACS Sens. 10 (2025) 8839–8851.
[84] D. Ji, B. Li, D. Zhang, B.T. Raj, M.d. Rezeq, W. Cantwell, L. Zheng, A multifunctional MXene/PVA hydrogel as a continuous ionic thermoelectric generator and a strain/temperature sensor, Small 21 (2024) 2407529.
[85] W. Gao, J. Chang, X. Li, S. Li, Y. Zhou, X. Hou, L. Long, J. Zhao, X. Yuan, A quenched double-hydrophilic coating for the enhancement of water retention of hydrogels, Adv. Funct. Mater. 33 (2023) 2303306.
[86] H. Yuan, T. Zhu, Y. Huang, Z. Wang, P. Han, L. Tan, J. Wu, X. Chen, P. Yao, C. Zhu, et al., Hydrophobic and adhesive elastomer encapsulation for anti-drying, non-swelling, and adhesive hydrogels, Adv. Funct. Mater. 34 (2024) 2409703.
[87] Y. Lu, Y. Yue, Q. Ding, C. Mei, X. Xu, S. Jiang, S. He, Q. Wu, H. Xiao, J. Han, Environment-tolerant ionic hydrogel–elastomer hybrids with robust interfaces, high transparence, and biocompatibility for a mechanical–thermal multimode sensor, Infomat. 5 (2023) e12409.
[88] P. Panda, P. Maity, A. Dutta, R.K. Das, Anisotropic anti-swelling hydrogels with hydrophobic association and metal–ligand cross-links for applications in underwater strain sensing and anisotropic actuation, Langmuir 41 (2025) 13301–13314.
[89] Y. Huang, C. Kong, C. Li, X. Li, J. Shi, H. Wang, S. Jiang, X. Xiong, K. Wu, L. Yang, Anti-swelling hydrogels via metal coordination network for underwater motion sensors and wireless electronic devices, J. Mater. Chem. C 12 (2024) 19281–19295.
[90] J. Wu, Z. Pan, Z.Y. Zhao, M.H. Wang, L. Dong, H.L. Gao, C.Y. Liu, P. Zhou, L. Chen, C.J. Shi, et al., Anti-swelling, robust, and adhesive extracellular matrix-mimicking hydrogel used as intraoral dressing, Adv. Mater. 34 (2022) 2200115.
[91] R. Wu, T. Zhu, Y. Ni, C. Wu, W. Wang, K. Zhao, J. Huang, Y. Lai, UV-cured dense double network hydrogel via multiple dynamic crosslinking for stable amphibious motion sensing, Adv. Funct. Mater. 36 (2025) e15120.
[92] Y. Fu, C. Yang, B. Zhang, Z. Wan, S. Wang, K. Zhang, L. Yang, R. Wei, A highly sensitive, conductive, and flexible hydrogel sponge as a discriminable multimodal sensor for deep-learning-assisted gesture language recognition, Adv. Funct. Mater. 35 (2024) 2416453.
[93] R.J. DeVolder, Y. Seo, H. Kong, Proangiogenic alginate-g-pyrrole hydrogel with decoupled control of mechanical rigidity and electrically conductivity, Biomater. Res. 21 (2017) s40824-017-0110-x.
[94] P. He, J. Wu, X. Pan, L. Chen, K. Liu, H. Gao, H. Wu, S. Cao, L. Huang, Y. Ni, Anti-freezing and moisturizing conductive hydrogels for strain sensing and moist-electric generation applications, J. Mater. Chem. A 8 (2020) 3109–3118.
[95] M.S. Rahman, A. Shon, R. Joseph, A. Pavlov, A. Stefanov, M. Namkoong, H. Guo, D. Bui, R. Master, A. Sharma, et al., Soft, stretchable conductive hydrogels for high-performance electronic implants, Sci. Adv. 11 (2025) ads4415.
[96] K. Zhang, Y. Pang, C. Chen, M. Wu, Y. Liu, S. Yu, L. Li, Z. Ji, J. Pang, Stretchable and conductive cellulose hydrogel electrolytes for flexible and foldable solid-state supercapacitors, Carbohydr. Polym. 293 (2022) 119673.
[97] Y. Shi, R. Wang, S. Bi, M. Yang, L. Liu, Z. Niu, An anti-freezing hydrogel electrolyte for flexible zinc-ion batteries operating at −70°C, Adv. Funct. Mater. 33 (2023) 2214546.
[98] W. Zhu, S. Wang, Y. Lu, W. Yang, S. Ge, Z. Lou, S. He, S. Jiang, J. Han, High-toughness multifunctional conductive hydrogel fibers via microfluidic spinning for flexible strain sensor, Ind. Crop. Prod. 222 (2024) 119598.
[99] S. Li, J. Ma, C. Zhu, G. Chen, J. Han, J. Fu, Anisotropic tough and non-swelling hydrogels based on Hofmeister-effect for underwater monitoring, Adv. Funct. Mater. 36 (2026) e27007.
[100] Y. Li, X. Wei, F. Jiang, Y. Wang, M. Xie, J. Peng, C. Yi, J. Li, M. Zhai, An ultrastretchable and highly conductive hydrogel electrolyte for all-in-one flexible supercapacitor with extreme tensile resistance, Energy Environ. Mater. 8 (2024) e12820.
[101] J. Ma, C. Zheng, Y. Lu, Y. Yue, W. Yang, C. Mei, X. Xu, H. Xiao, J. Han, Mussel-adhesive chemistry inspired conductive hydrogel with self-adhesion, biocompatibility, self-recovery and fatigue-resistance performances as flexible sensing electronics, Compos. A: Appl. Sci. Manuf. 185 (2024) 108330.
[102] J. Ma, W. Yang, J. Chen, Y. Zhou, M. Ye, X. Xu, H. Xiao, J. Han, Lignosulfonate-enhanced dispersion and compatibility of liquid metal nanodroplets in PVA

hydrogel for improved self-recovery and fatigue resistance in wearable sensors, Int. J. Biol. Macromol. 306 (2025) 141653.
[103] C. Sang, S. Wang, X. Jin, X. Cheng, H. Xiao, Y. Yue, J. Han, Nanocellulose-mediated conductive hydrogels with NIR photoresponse and fatigue resistance for multifunctional wearable sensors, Carbohydr. Polym. 333 (2024) 121947.
[104] C. Zheng, J. Ma, Y. Lu, M. Ye, Y. Zhou, W. Yang, S. He, S. Jiang, H. Xiao, J. Han, Nanocellulose-mediated double-network conductive organohydrogels with self-adhesive, biocompatible and environmentally tolerant properties for wearable biosensors, Carbohydr. Polym. 363 (2025) 123732.
[105] J. Ma, S. Li, Y. Gu, D. Wang, W. Yang, C. Mei, X. Xu, H. Xiao, J. Han, Innovative cellulose-mediated liquid metal composites hydrogel with adhesive and mechanical-thermal multimodal sensing capabilities for smart wearable devices, Chem. Eng. J. 530 (2026) 173583.
[106] A. Chae, G. Murali, S.Y. Lee, J. Gwak, S.J. Kim, Y.J. Jeong, H. Kang, S. Park, A. S. Lee, D.Y. Koh, et al., Highly oxidation-resistant and self-healable MXene-based hydrogels for wearable strain sensor, Adv. Funct. Mater. 33 (2023) 2213382.
[107] Y. Bai, X. Li, Y. Shi, Y. Zhang, S. Xie, Slide-ring based hydrogel sensors with extreme wide temperature adaptability toward winter swimming sensing application, Small 21 (2025) e08493.
[108] S. Zheng, A. Liu, X. Zhang, W. Wu, L. Chen, C. Lai, Y. Lai, K. Liu, Penguin skin-inspired, nanoparticle-reinforced hydrogels for extreme environment-resistant piezoionic generation and sensing, Adv. Funct. Mater. 36 (2025) e14944.
[109] L. Zhao, Q. Ling, X. Fan, H. Gu, Self-healable, adhesive, anti-drying, freezing-tolerant, and transparent conductive organohydrogel as flexible strain sensor, triboelectric nanogenerator, and skin barrier, ACS Appl. Mater. Interfaces 15 (2023) 20975–40990.
[110] H. Jung, D. Lee, K. Kim, H. Choi, S. An, Y. Lee, S. Lee, J. Yoon, D. Seong, Y. Kim, et al., Hydrogel–elastomer-based conductive nanomembranes for soft bioelectronics, Nat. Nanotechnol. 20 (2025) 1822–1830.
[111] Z. Lv, J. Liu, K. Shen, M. Zhang, Z. Liu, Y. Li, R. Xie, J. Liu, J. Zhu, Y. Cheng, Elastic polymeric hydrogels via sparse chain entanglements and hydrophobic aggregates, Adv. Funct. Mater. 36 (2025) e23406.
[112] Y. Ma, Y. Lu, Y. Yue, S. He, S. Jiang, C. Mei, X. Xu, Q. Wu, H. Xiao, J. Han, Nanocellulose-mediated bilayer hydrogel actuators with thermo-responsive, shape memory and self-sensing performances, Carbohydr. Polym. 335 (2024) 122067.
[113] Y. Lu, Y. Ma, F. Deng, Y. Yue, S. Jiang, Q. Wu, H. Xiao, J. Han, Gradient wood-derived hydrogel actuators constructed by an isotropic-anisotropic structure strategy with rapid thermal-response, high strength and programmable deformation, Chem. Eng. J. 504 (2025) 158903.
[114] Y. Lu, S. Li, F. Deng, Y. Yue, S. He, S. Jiang, M. Ye, Y. Zhou, H. Xiao, J. Han, Programmable and multi-stimuli responsive hydrogel actuator mediated by nanocellulose with intrinsic self-sensing capacity, Carbohydr. Polym. 371 (2026) 124527.
[115] S. Li, J. Ma, J. Han, J. Fu, Biomimetic self-sensing hydrogel soft robotics: precise structures for integrated actuation and sensing, Adv. Funct. Mater. 36 (2026) e74884.
[116] J. Ma, Y. Gu, D. Wang, W. Yang, et al., A comprehensive review of lignocellulose-liquid metal composites: from synthesis strategies to emerging applications, Mater. Today 97 (2026) 103370.
[117] E. Liu, S. Cheng, Q. Zhao, S. Lin, X. Mei, Injectable, self-healing, superadhesive PVA hydrogels promote skin wound healing by regulating the inflammatory microenvironment, ACS Appl. Bio Mater. 8 (2025) 5120–5128.